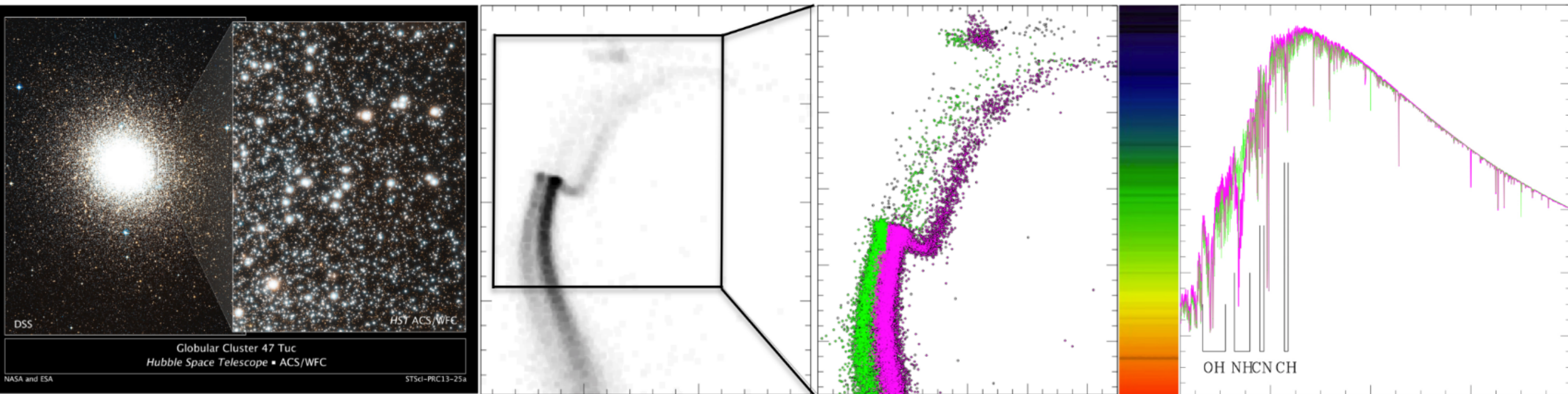


Spectroscopy of stellar populations

Antonino P. Milone



Most-relevant stellar parameters

Effective temperature T_{eff} = T_{BB} with same L and R as the real star

$$L = 4\pi R^2 \sigma T_{\text{eff}}^4$$

Surface gravity $\log g$ usually expressed in cgs units and as \log_{10}

$$g = GM/R^2$$

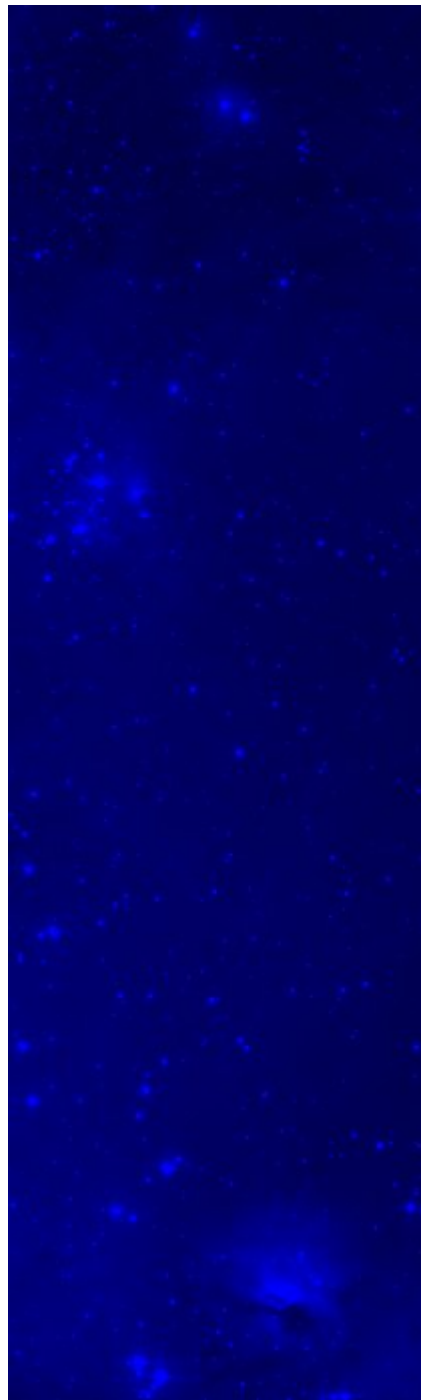
Metallicity Z or [Fe/H] $Z = \frac{\text{mass (elements heavier than He)}}{\text{total mass (unit volume)}} \approx 0.018$ Sun

$$[\text{Fe}/\text{H}] = \log [N(\text{Fe})/N(\text{H})]_* - \log [N(\text{Fe})/N(\text{H})]_{\text{Sun}}$$

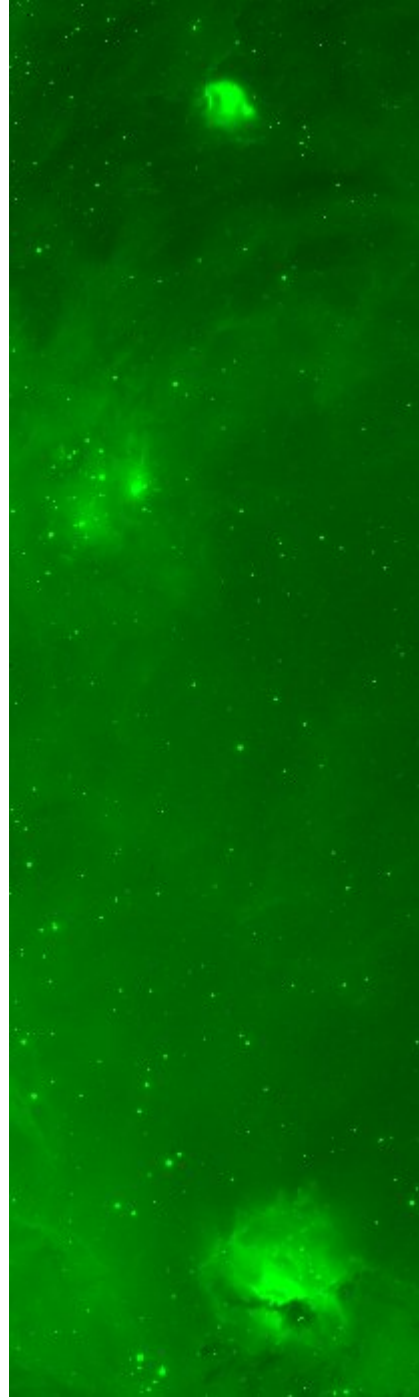
$$[\alpha/\text{Fe}] = \log [N(\alpha)/N(\text{Fe})]_* - \log [N(\alpha)/N(\text{Fe})]_{\text{Sun}}$$

where α is an « α -element », i.e. with a nucleus made of an integer number of α -particles

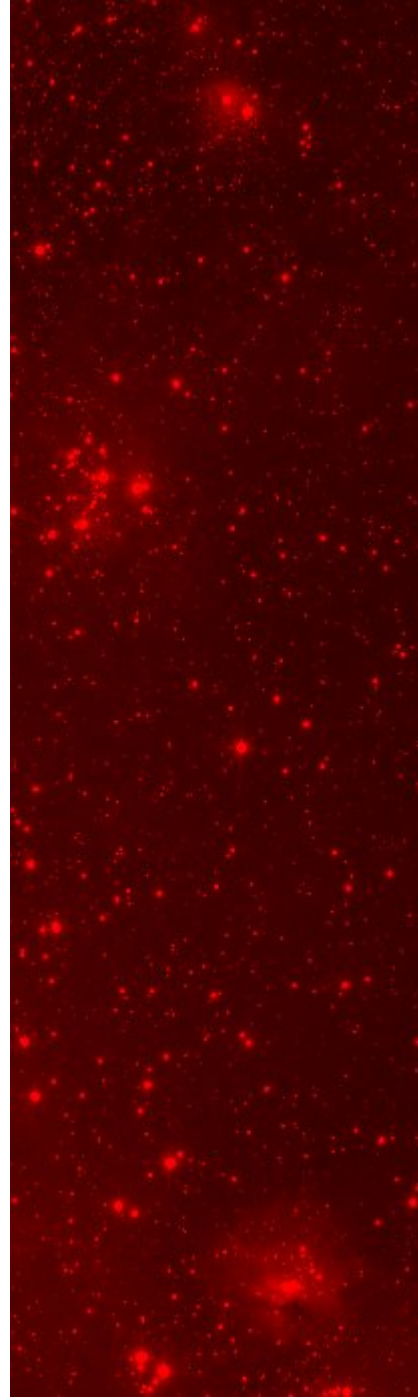
Multi-band photometry



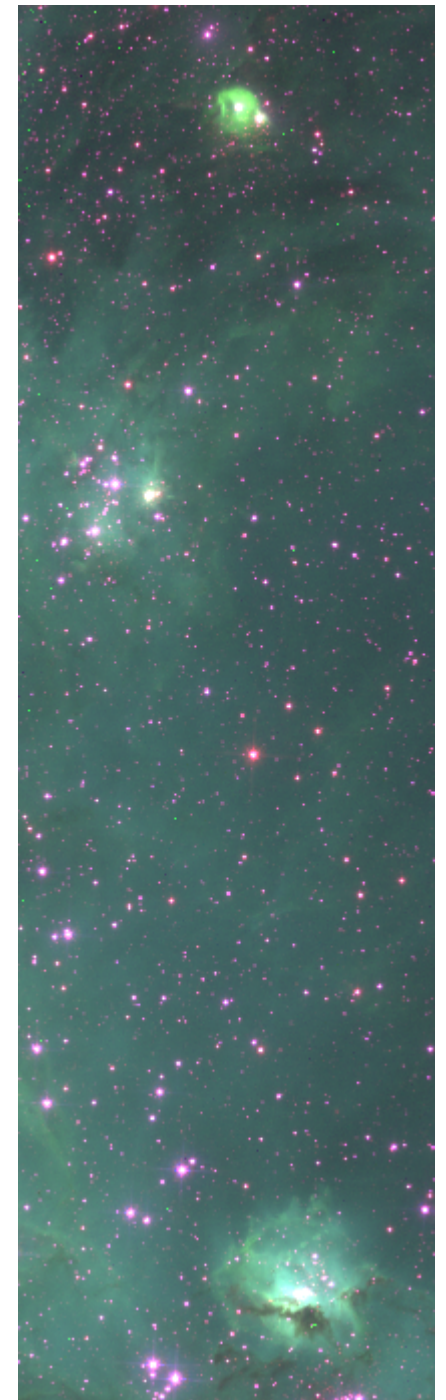
+



+



=

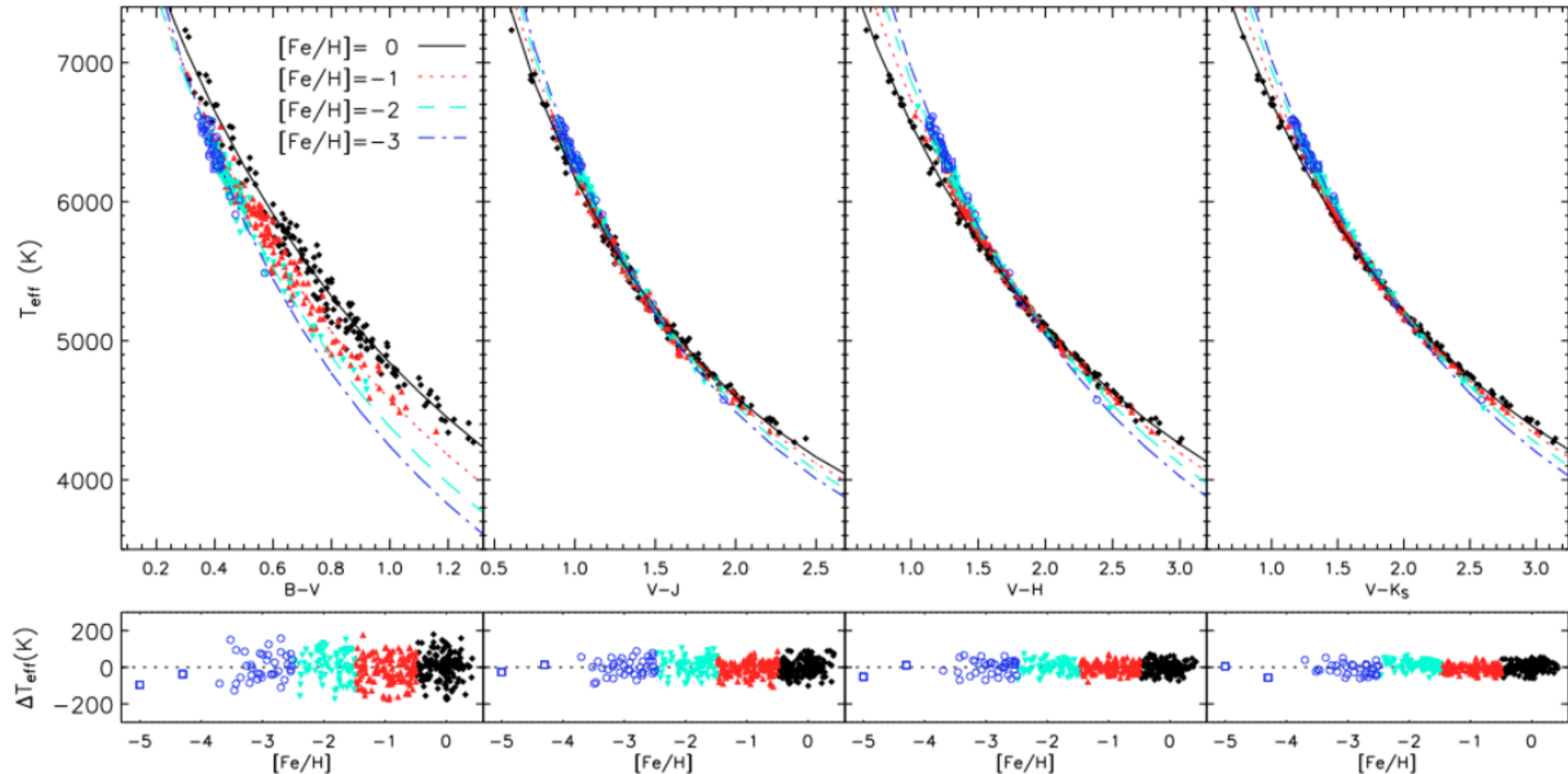


Multi-band photometry



Multi-band photometry and stellar parameters

Photometry of stars with well-known stellar parameters provide **empirical T_{eff} -color** relations.

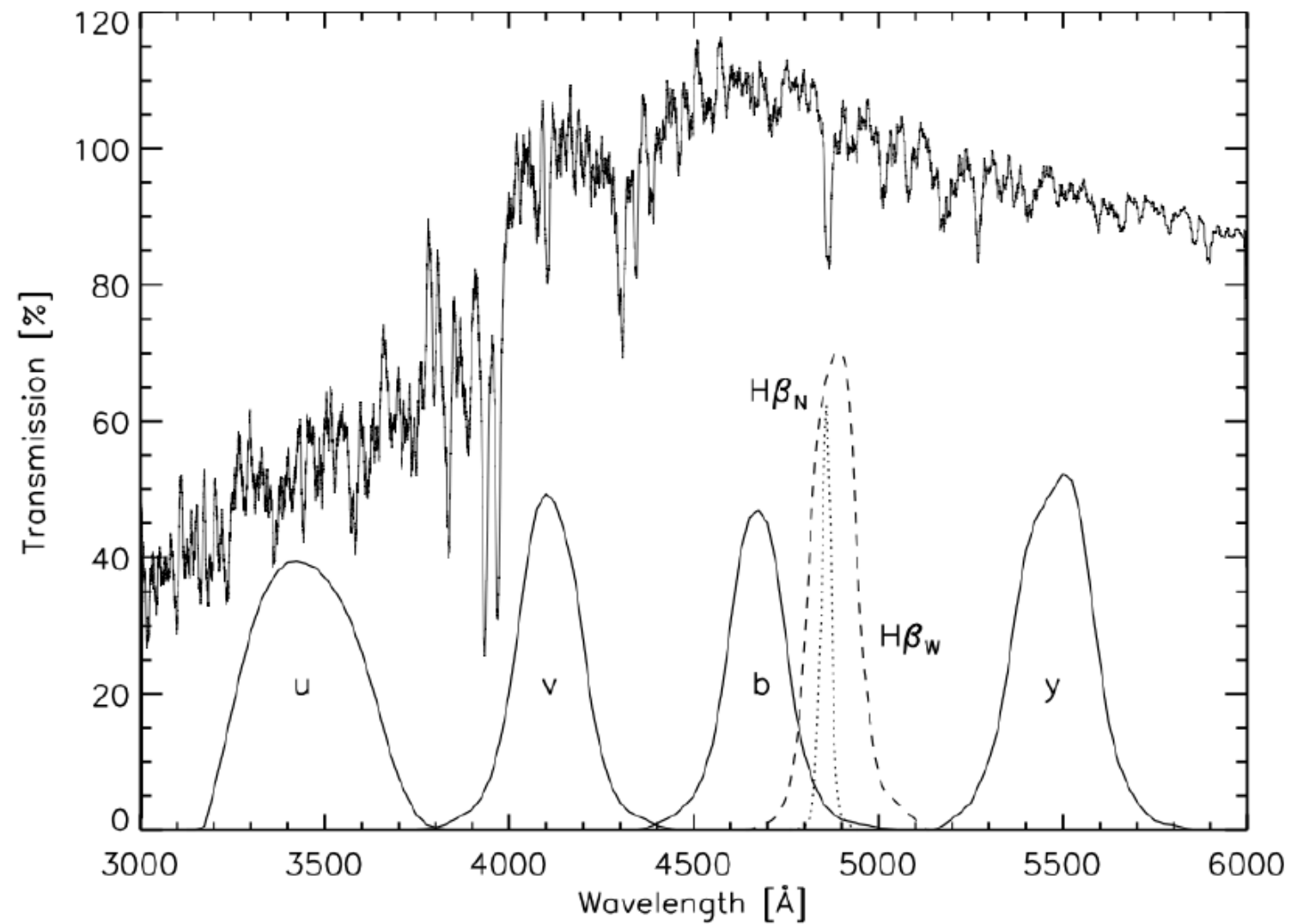


The relation depends on metallicity.

Reddening is a major issue for photometric parameters

Stroemgren photometry

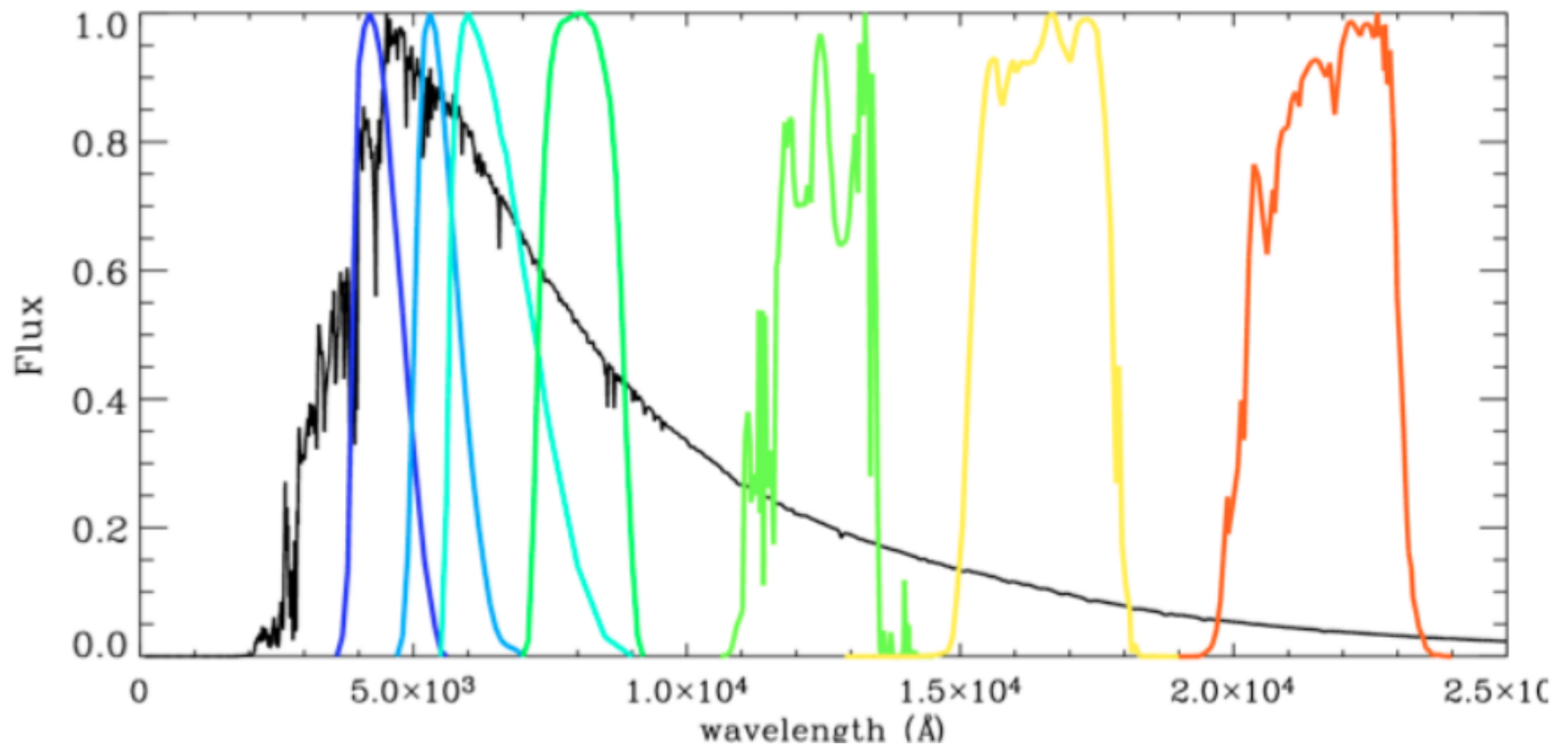
$(b - y)$	continuum slope	→	T_{eff}
$m_1 = (v - b) - (b - y)$	blanketing at 4100 Å	→	[Fe/H]
$c_1 = (u - v) - (v - b)$	Balmer discontinuity	→	log(g)
$\beta = \beta_w - \beta_n$	H β line	→	E(B-V)



Infrared flux method

It is based on the comparison between the monochromatic flux in the IR with the bolometric flux.

$$\frac{\mathcal{F}_{Bol}(\text{Earth})}{\mathcal{F}_{IR}(\text{Earth})} = \frac{\sigma T_{\text{eff}}^4}{\mathcal{F}_{IR}(\text{model})}$$

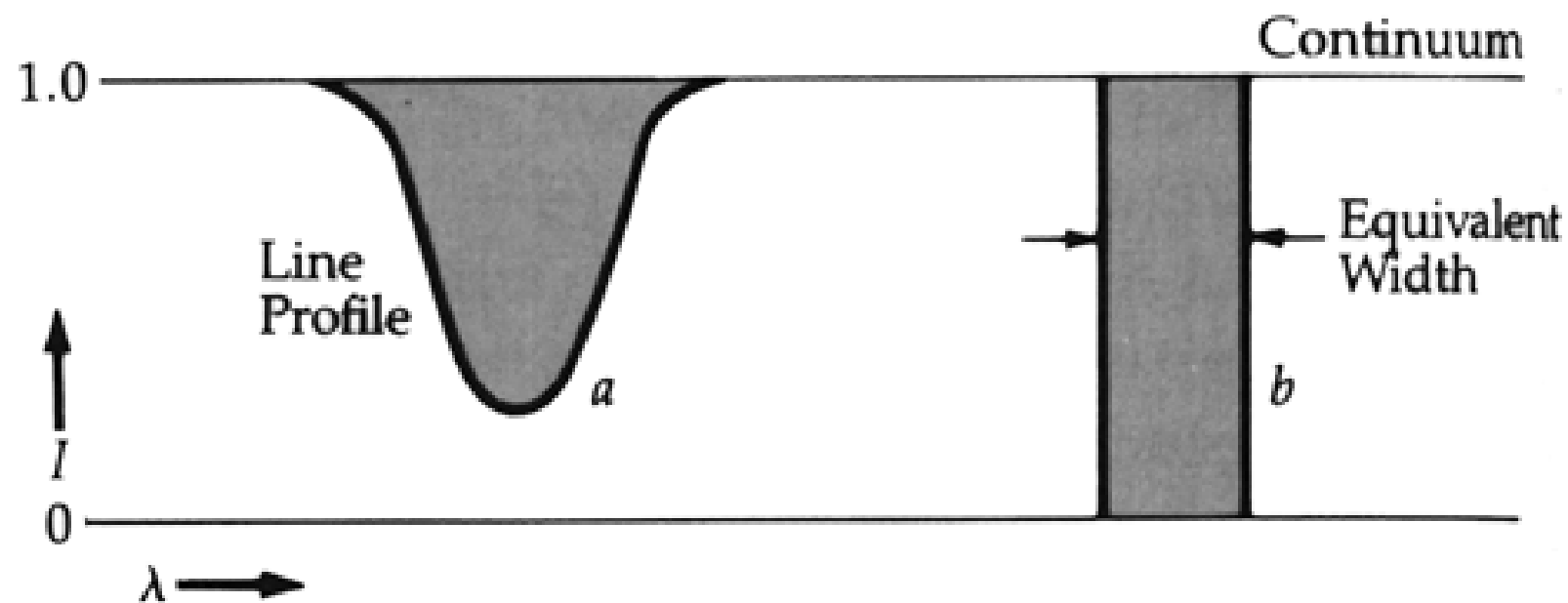


Casagrande et al. 2010

Measuring abundances: equivalent width

The equivalent width for an absorption/emission line is defined as the **width of a rectangle**

- whose **height** is equal to the height of the **continuous** and
- whose **area** is equal to the integrated area of the **line**.

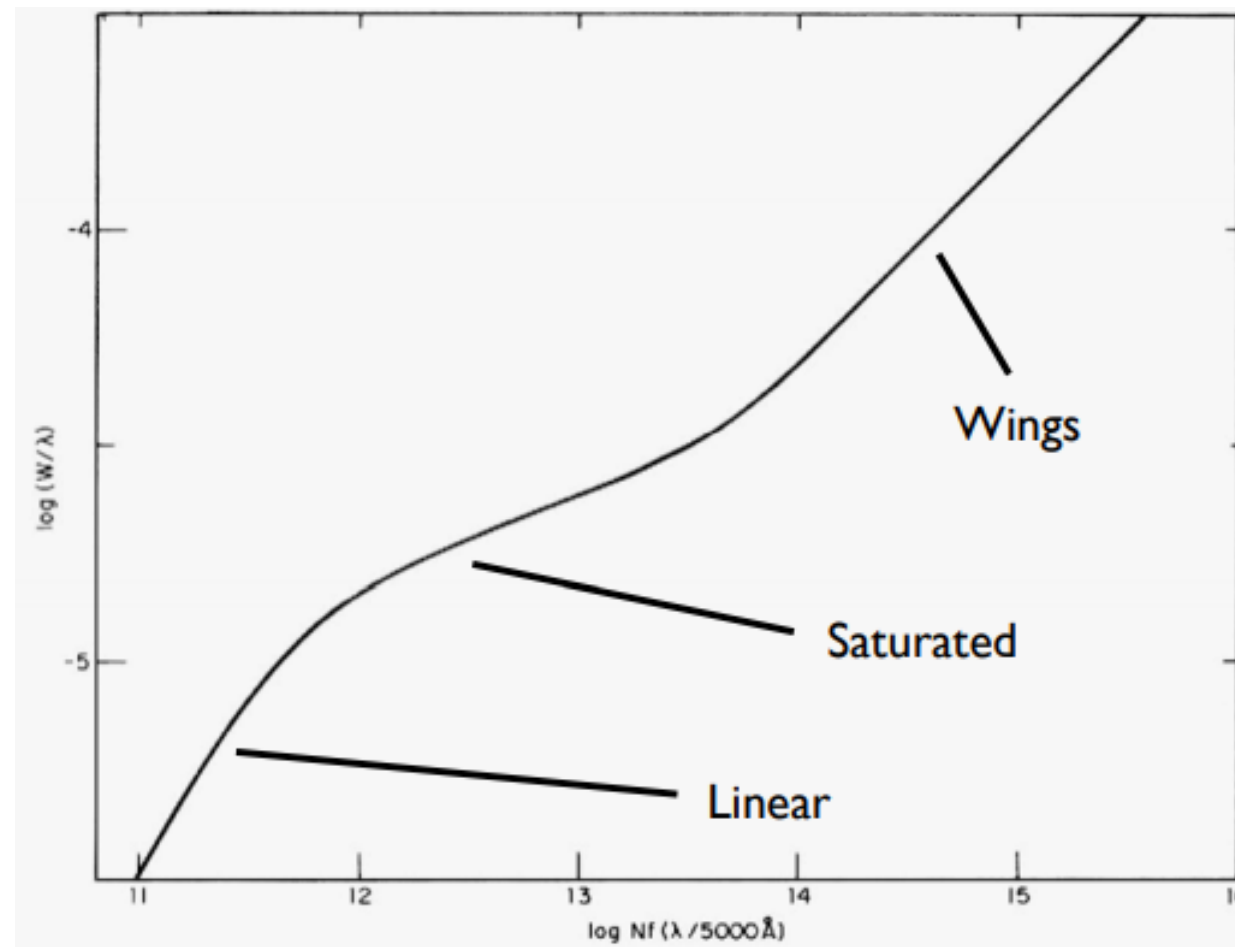


The equivalent width indicates the **strength** of a line.

The equivalent width is **independent** of the **shape** of the line and of the **instrumentation**.

Measuring abundances: equivalent width

The curve of growth describes the **equivalent width** of a spectral line as a function of the **column density** of the material from which the spectral line is observed.



It is used to infer the abundance of the gas making up the stellar atmosphere.

Measuring abundances: equivalent width

– **Weak lines:** Linear part. $W \propto A$

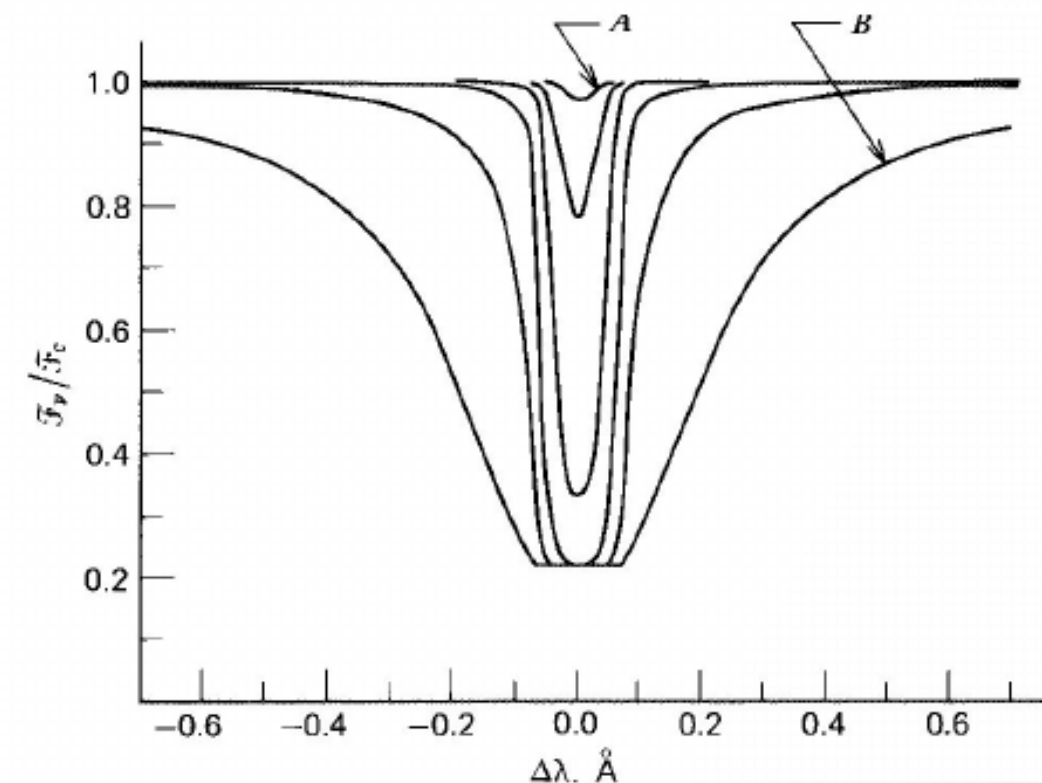
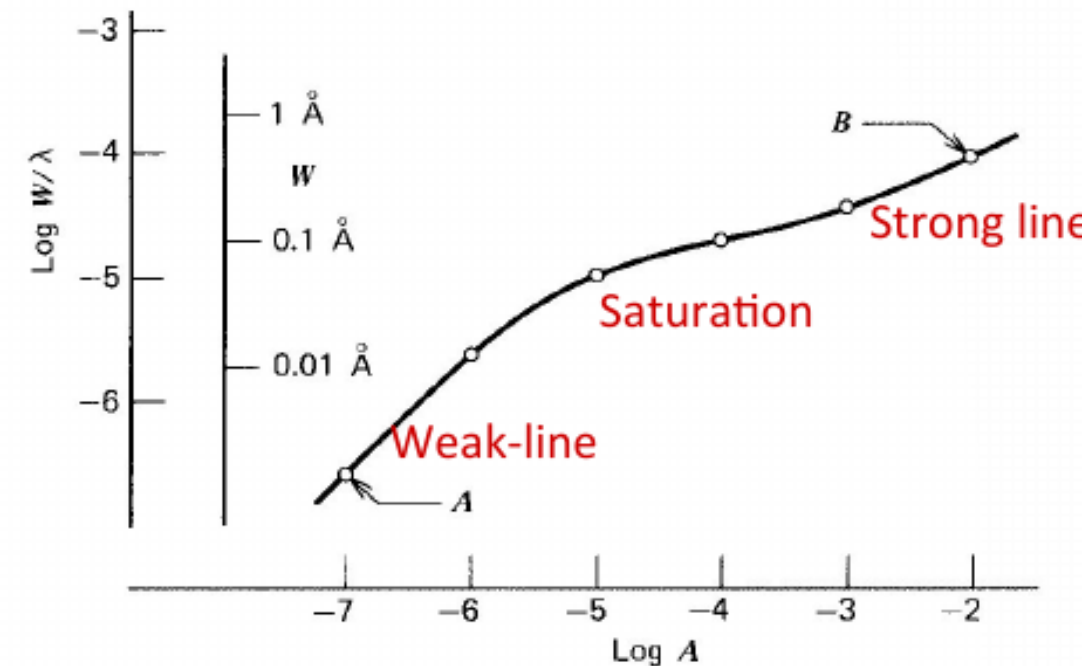
Doppler core dominates and the width is set by the thermal broadening $\Delta\lambda_D$. Depth of the line grows proportionally to abundance A

– **Saturation:** Plateau. $W \propto \sqrt{\log A}$

Doppler core approaches max. value and line saturates towards a constant value

– **Strong lines:** Wings dominate $W \propto \sqrt{A}$

optical depth in wings becomes significant
Strength depends on g_l



Measuring abundances: equivalent width

Obviously, one only gets the abundance of the particular ionization state and excitation level that produces the line.

The **Boltzmann** and **Saha** equations need to be applied then and the **pressure** and the **temperature** of the gas known to derive an abundance of the element (i.e. of all ionization states and excitation levels).



Saha distribution

Saha distribution for ionization population:

$$\frac{N_{i+1}}{N_i} = 2 \frac{1}{N_e} \frac{U_{i+1}}{U_i} \left(\frac{2\pi m_e kT}{h^2} \right)^{3/2} e^{-\chi_{ion}/kT}$$

χ_{ion} = ionization energy from state i to state $i+1$

N_e = number density of free electrons

Boltzmann distribution

Boltzmann distribution for excitation population:

$$\frac{n_u}{n_l} = \frac{g_u}{g_l} e^{-E_{ul}/kT}$$

$$\frac{n_l}{N_{total}} = \frac{g_l}{U(T)} e^{-\chi_l/kT}$$

$$U(T) = \sum_s g_s e^{-\chi_s/kT}$$

χ_l = excitation energy of level /

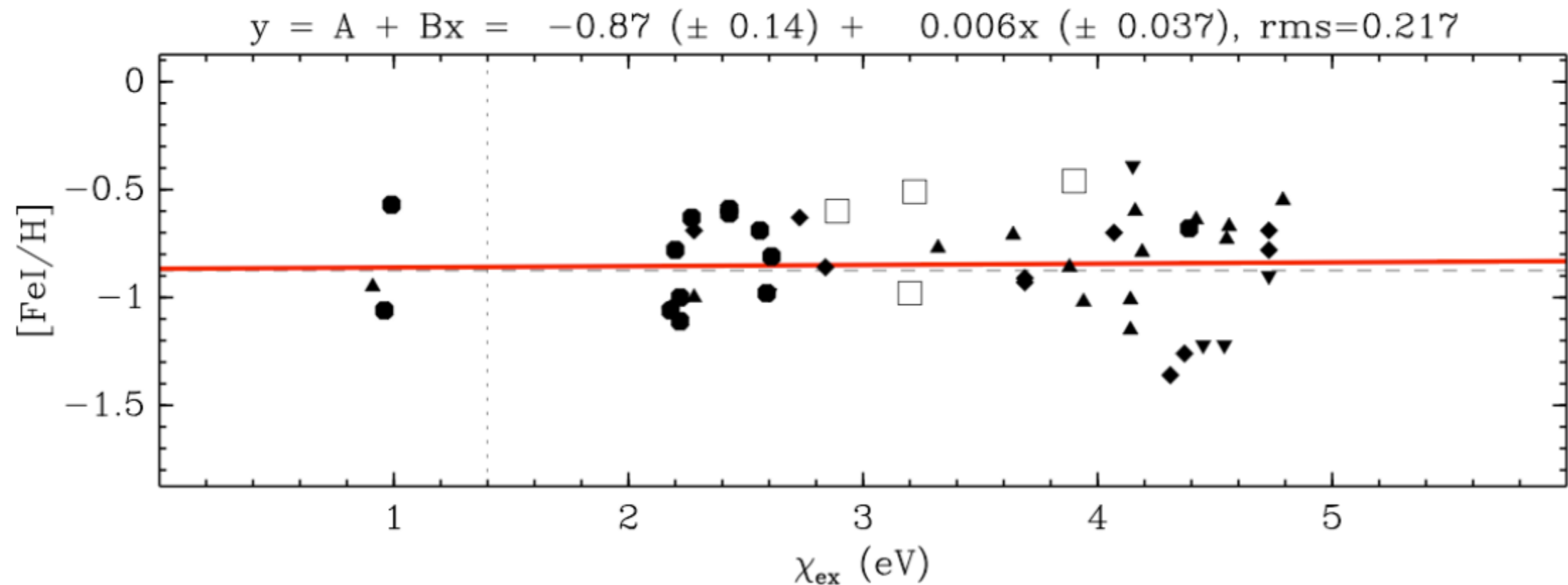
$U(T)$ = partition function

Temperature determination: Spectroscopy.

T_{eff} is determined such that the abundance of an element (usually Fe) is independent of the excitation potential (χ_{exc}) of the individual lines*

One needs many lines of a single element sampling a range of χ_{exc} \rightarrow iron

Final precision depends on spectral resolution, choice and number of lines and S/N ratios



* Boltzmann's equation under LTE conditions.

Source Letarte

log(g) determination: Spectroscopy.

Ionization balance:

Lines of **different ionization stages** (e.g. FeI, FeII) have different sensitivity to log(g).

E.g. in **cool** stars:

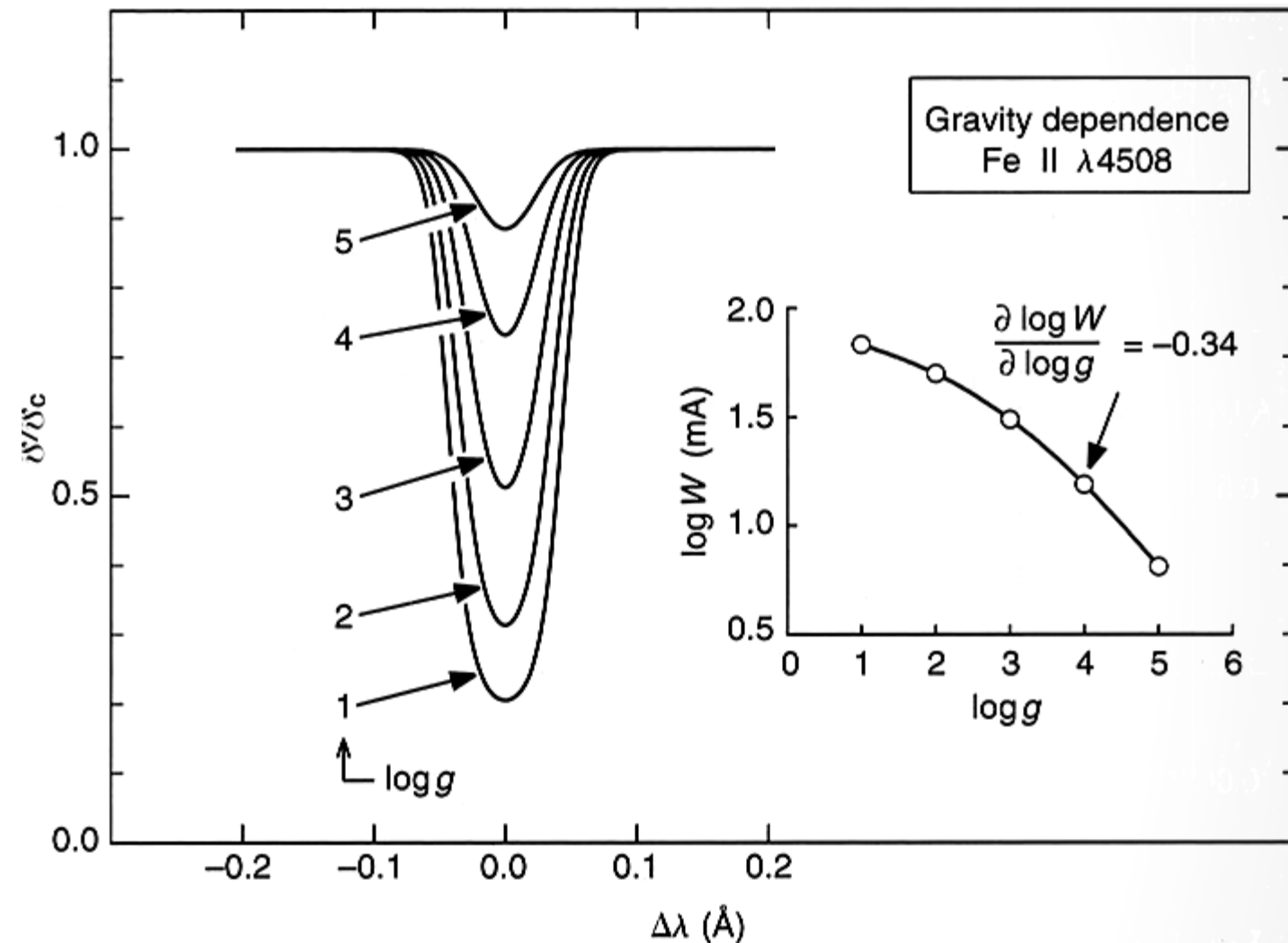
FeI, the dominant species:

$$g \uparrow \Rightarrow W_\lambda \approx$$

FeII, the minority species:

$$g \uparrow \Rightarrow W_\lambda \downarrow$$

By definition, gravity is related to $P_g \propto g^{2/3}$ and $P_e \propto g^{1/3}$

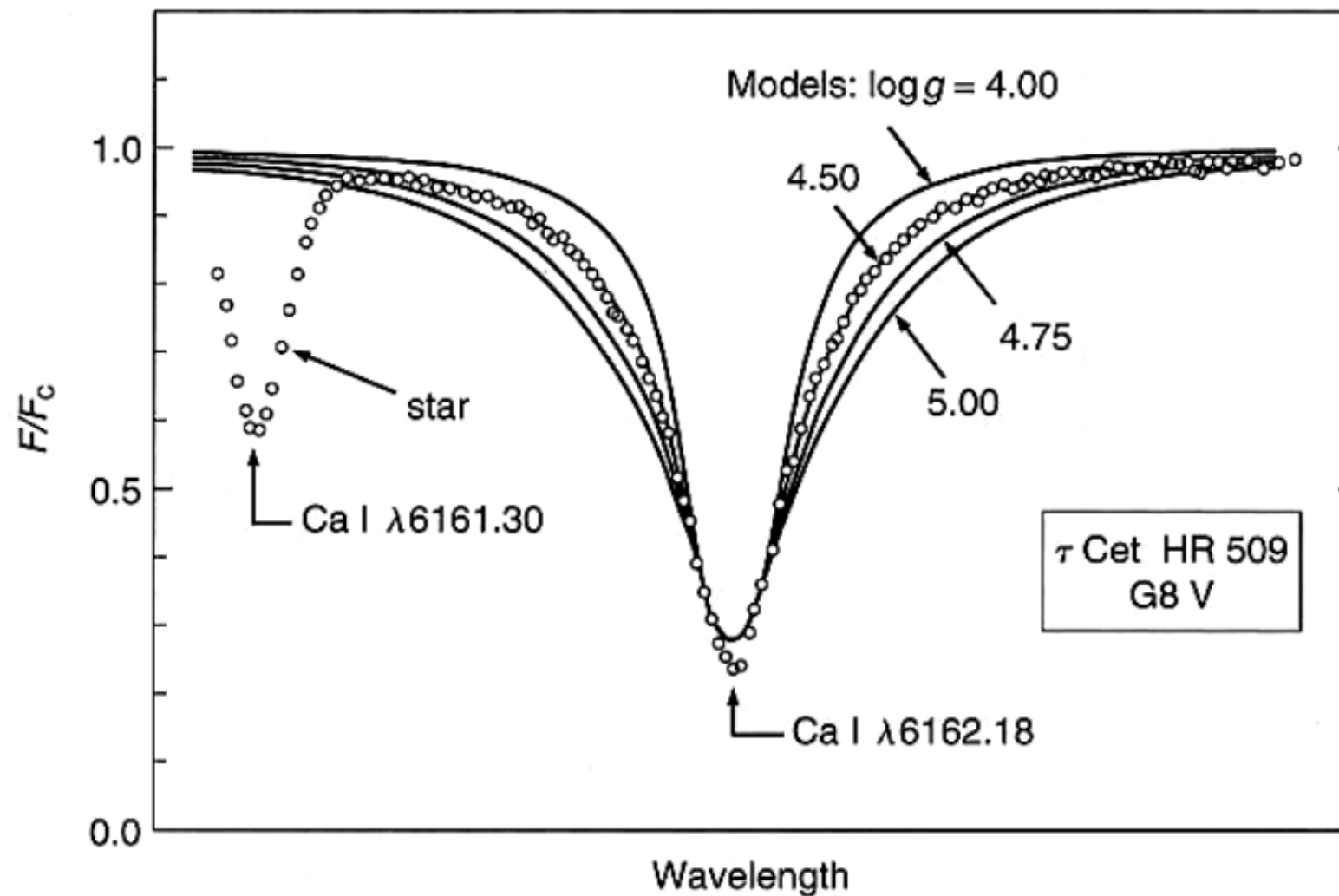


As a consequence, log(g) can be obtained by enforcing the **same abundance** is obtained from different ionization stages.

log(g) determination: Spectroscopy.

Strong lines

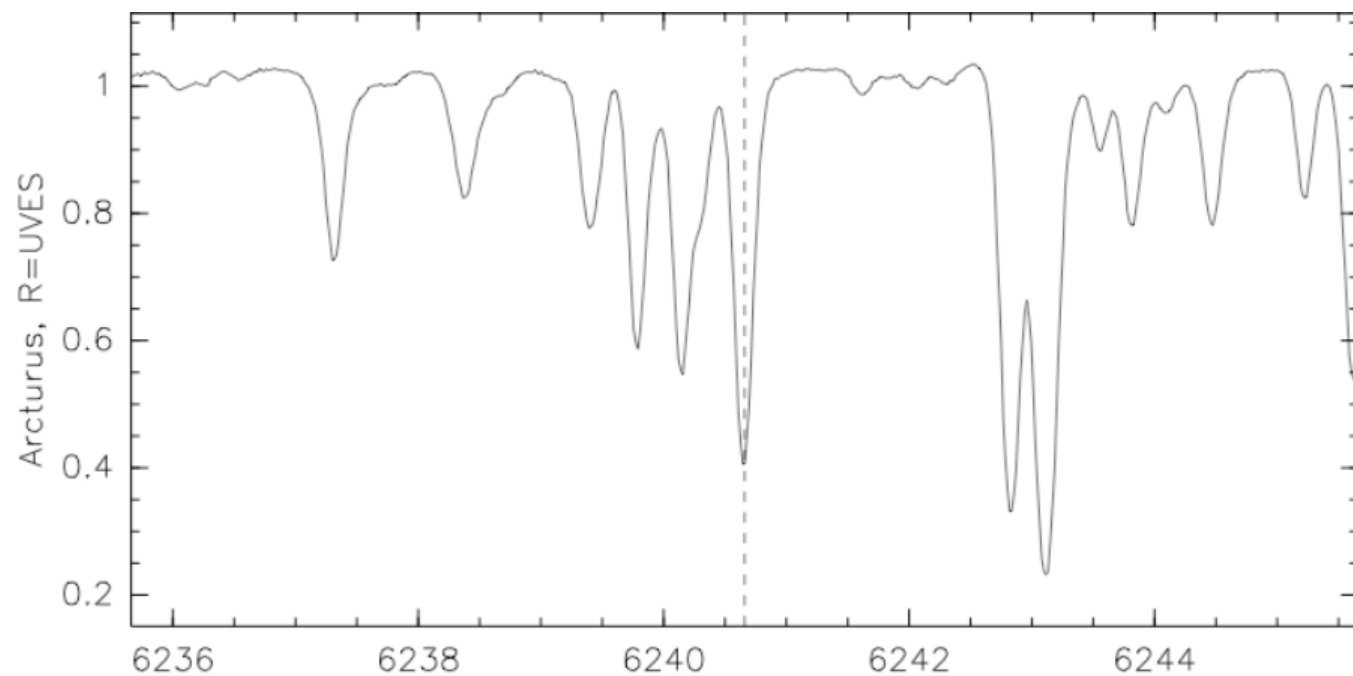
The wings of strong lines can depend on the atmospheric Pressure and thus on the surface gravity log(g).



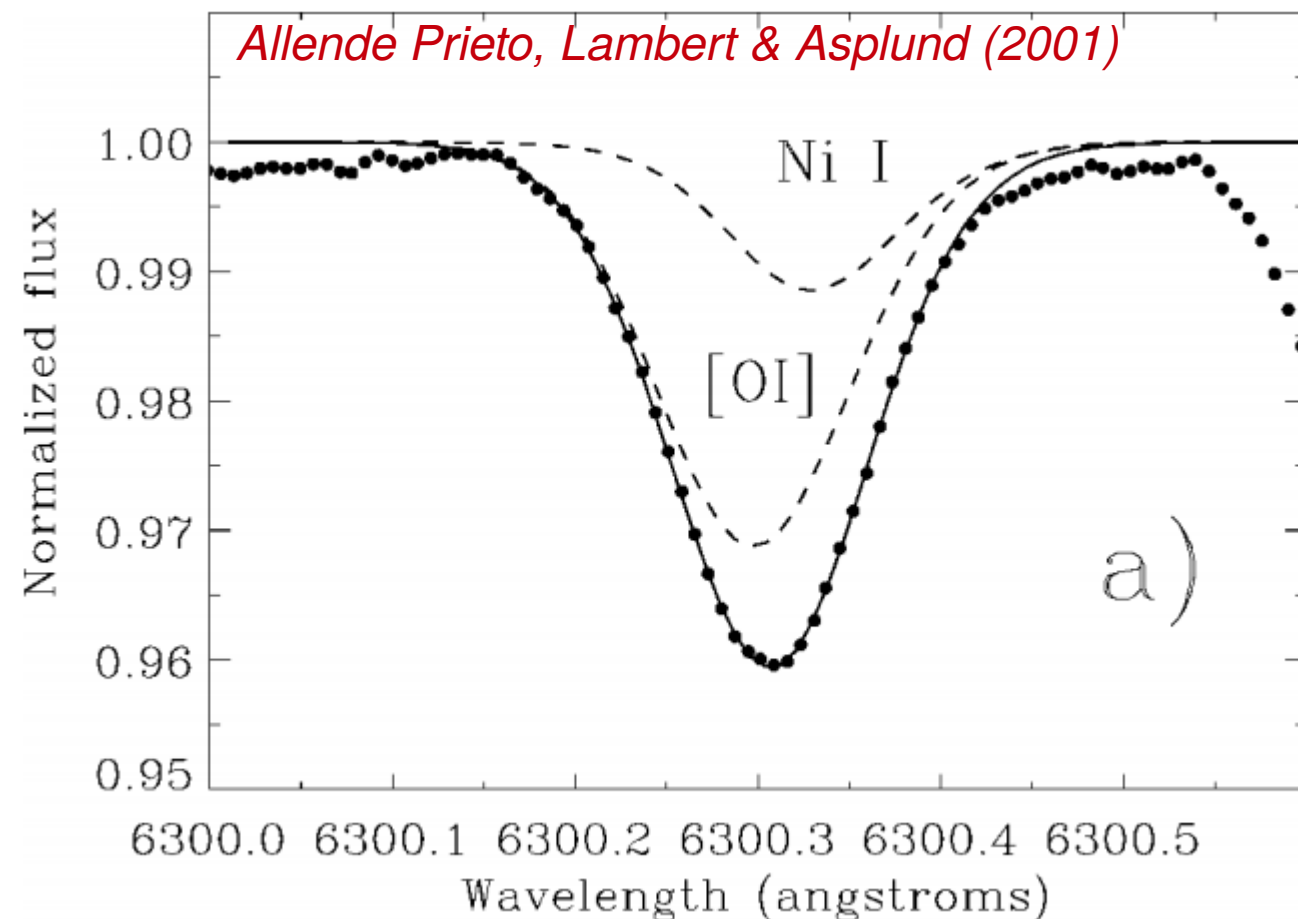
Note that the strength of wings depends also on effective temperature and on the abundance.

Spectra synthesis

- In real life, spectra are affected by **crowding and blends**.
- These represent major challenges for equivalent width determination...

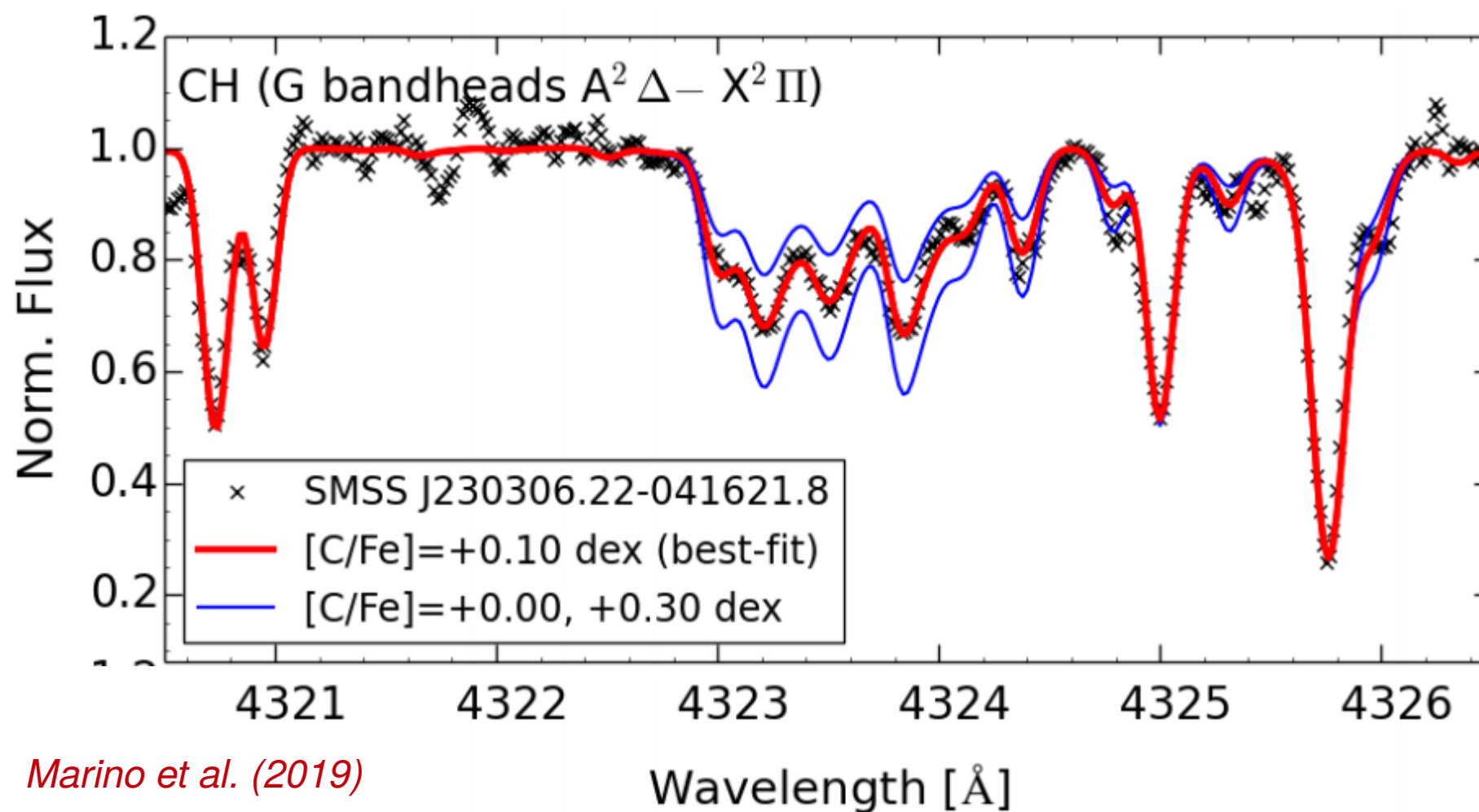


*Simulated spectrum of Arcturus (Resolution=UVES)
Source: F. Primas*



Spectral synthesis

Elemental abundances are often inferred by comparing the observed spectra with grids of **simulated spectra** with different chemical composition.



Marino et al. (2019)

Full spectral synthesis is required.

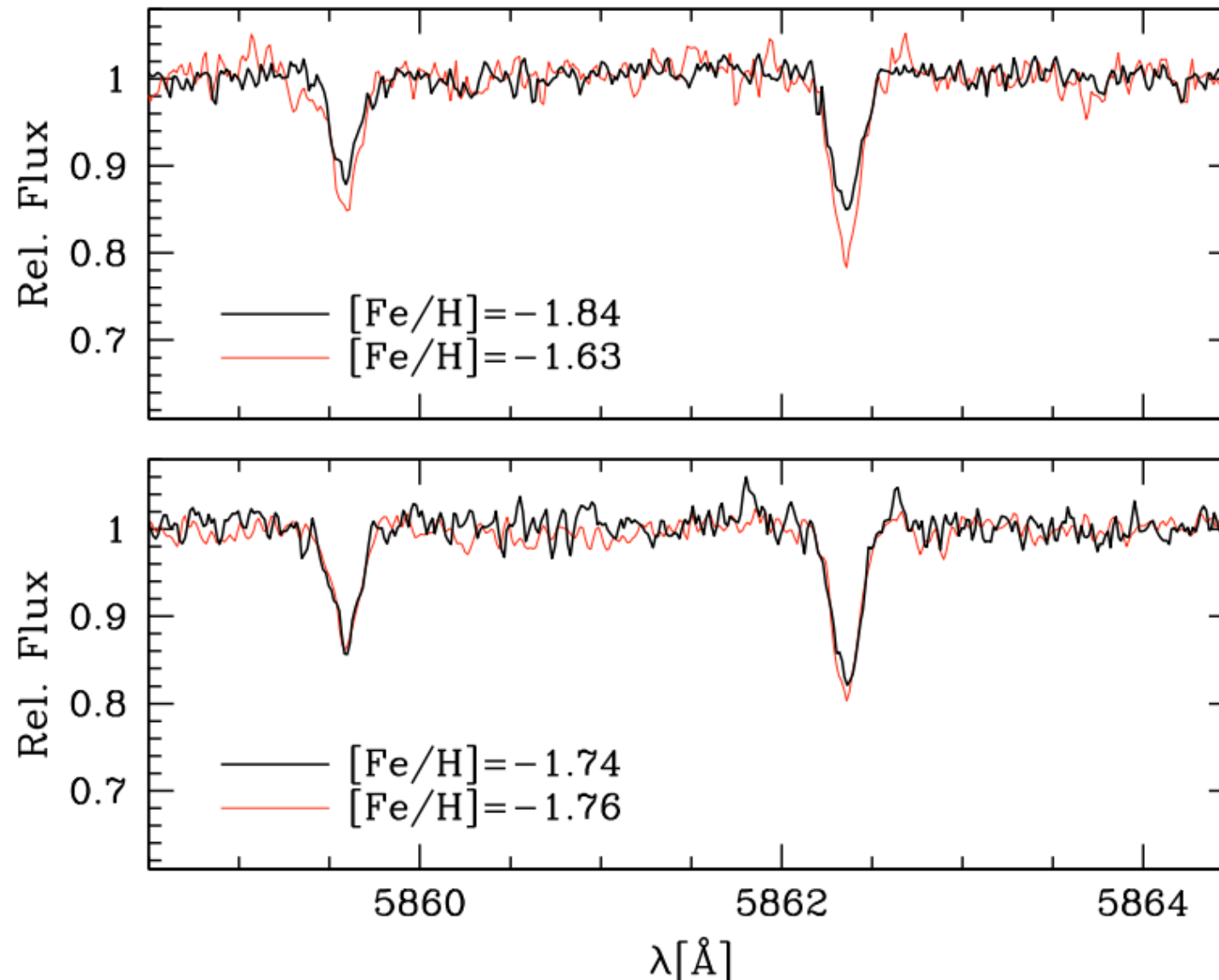
Uncertainties in parameters

The **typical** uncertainties in the estimated stellar parameters for late-type stars are:

- **T_{eff}** $\sim 100\text{-}300$ K (absolute error)
 $\sim 10\text{-}50$ K (relative error)
- **$\log(g)$** $\sim 0.1\text{-}0.3$ dex (strong lines)
 $\sim 0.1\text{-}1.0$ dex (ionization balance)
- **$[\text{Fe}/\text{H}]$** $\sim 0.1\text{-}0.5$ dex

Uncertainties larger for giants and metal-poor stars than for Sun. Note: all methods have at least a minor dependence also on the other parameters. An iterative procedure to determine the stellar parameters is therefore necessary.

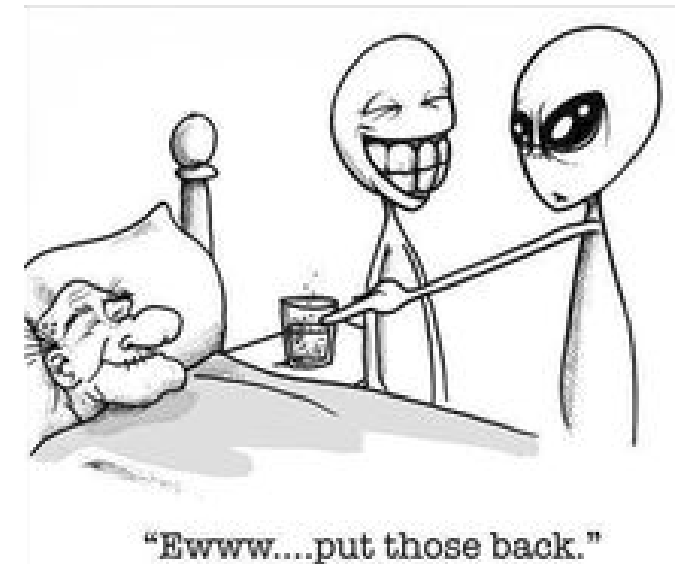
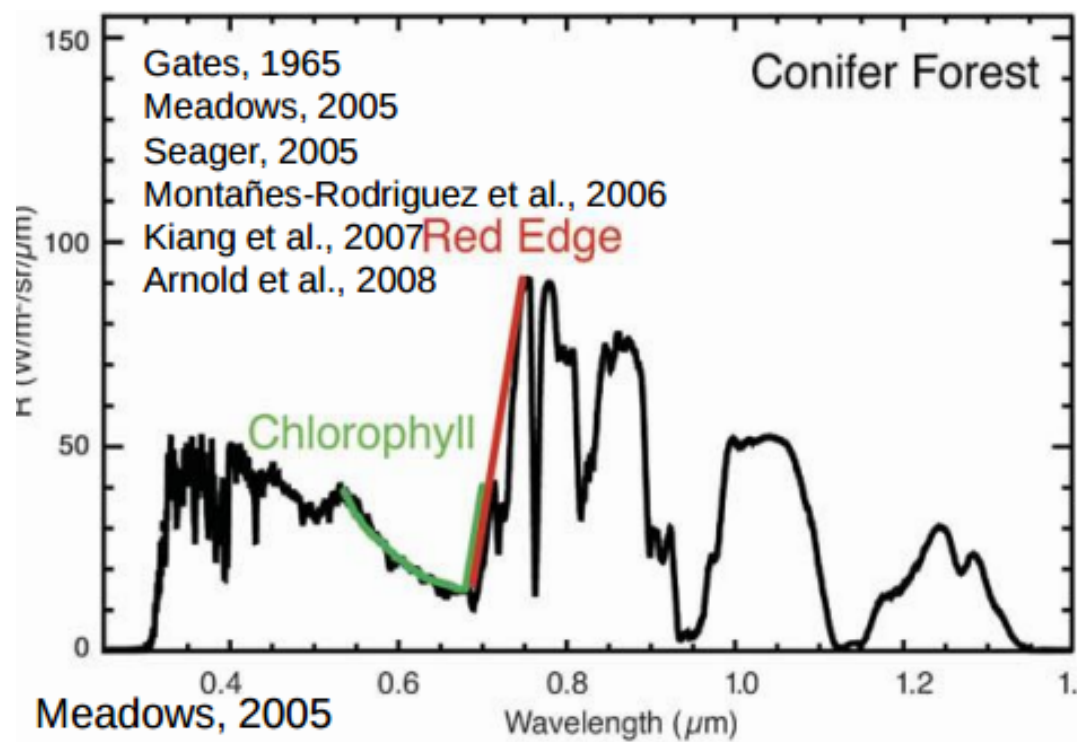
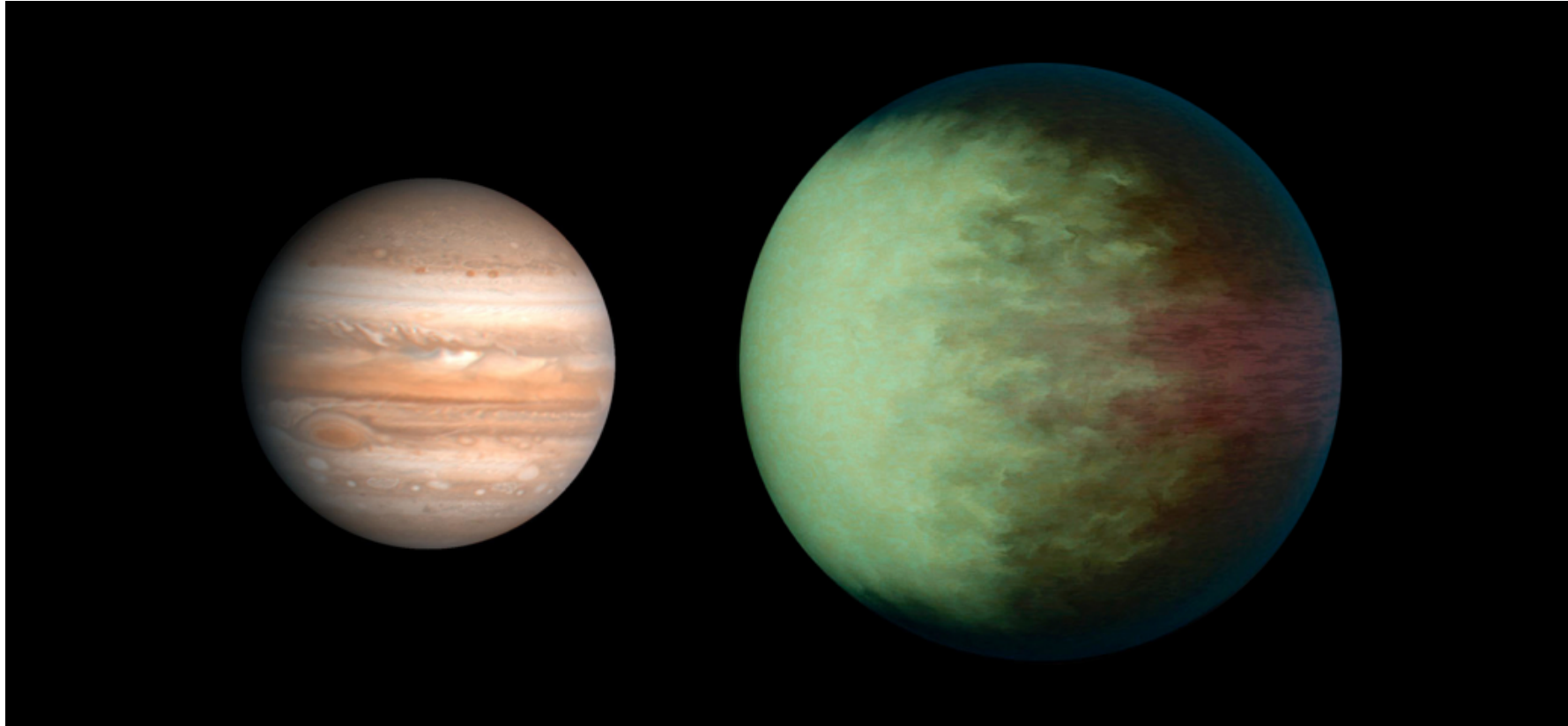
Relative abundances



Spectra of two couple of stars in the Globular Cluster M22 with similar atmospheric parameters. Marino et al. (2009)

The comparison between spectra of stars with the same atmospheric parameters allows us to detect very-small abundance differences.

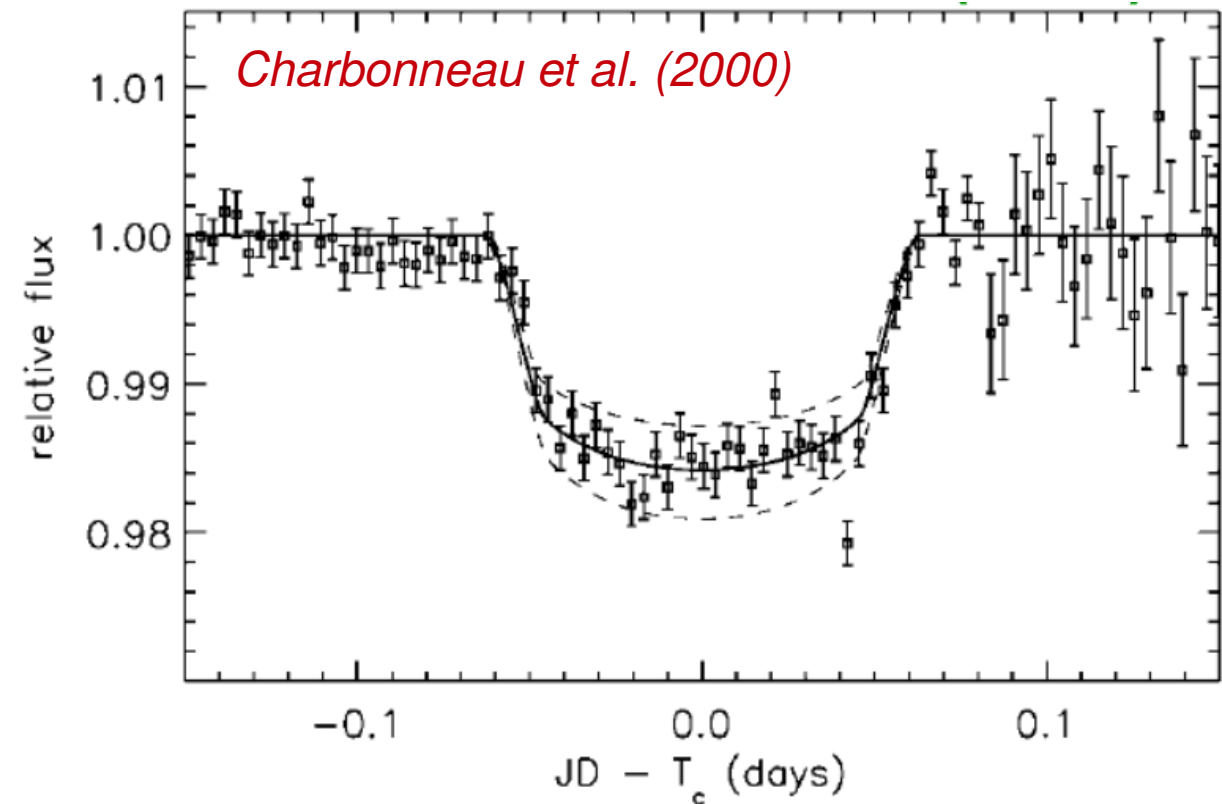
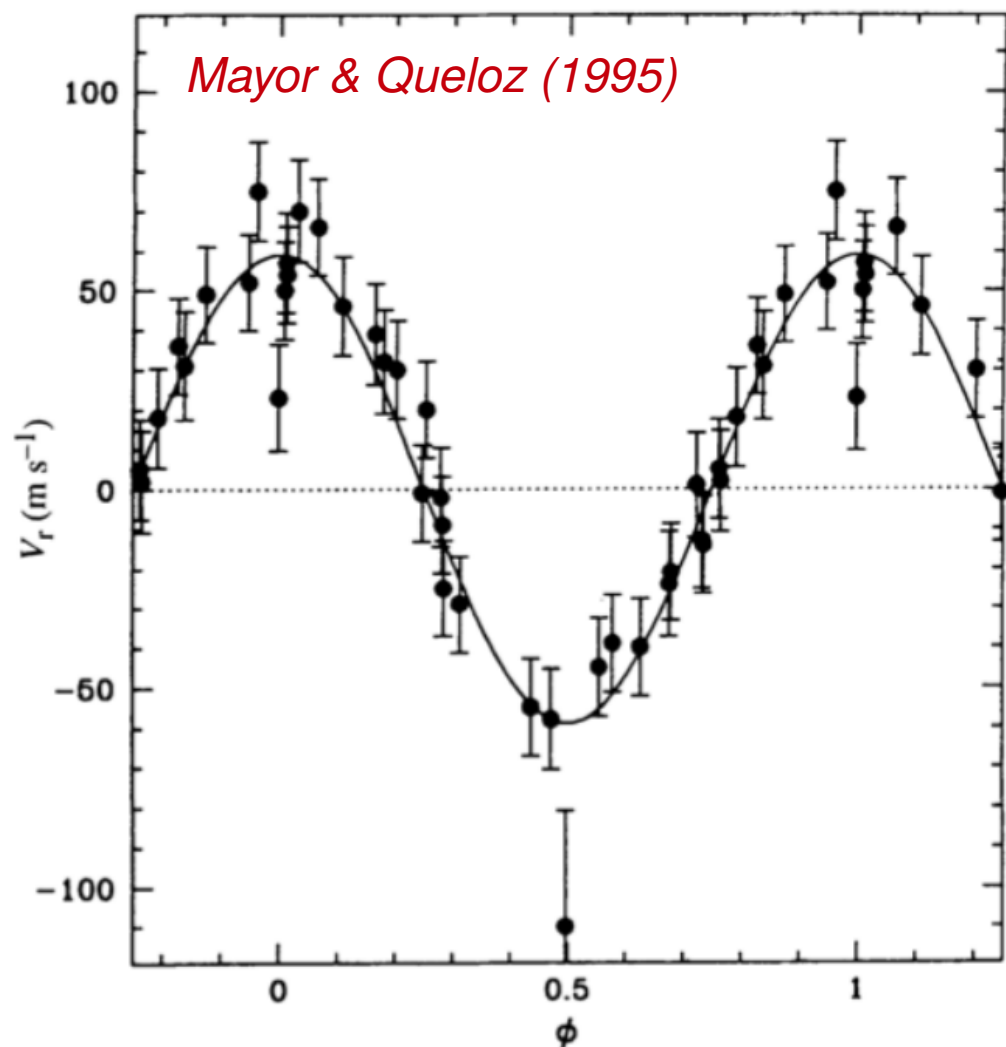
Application: Exoplanets



Application: Exoplanets

More than 3,700 extrasolar planets known (updated as in March 2018):

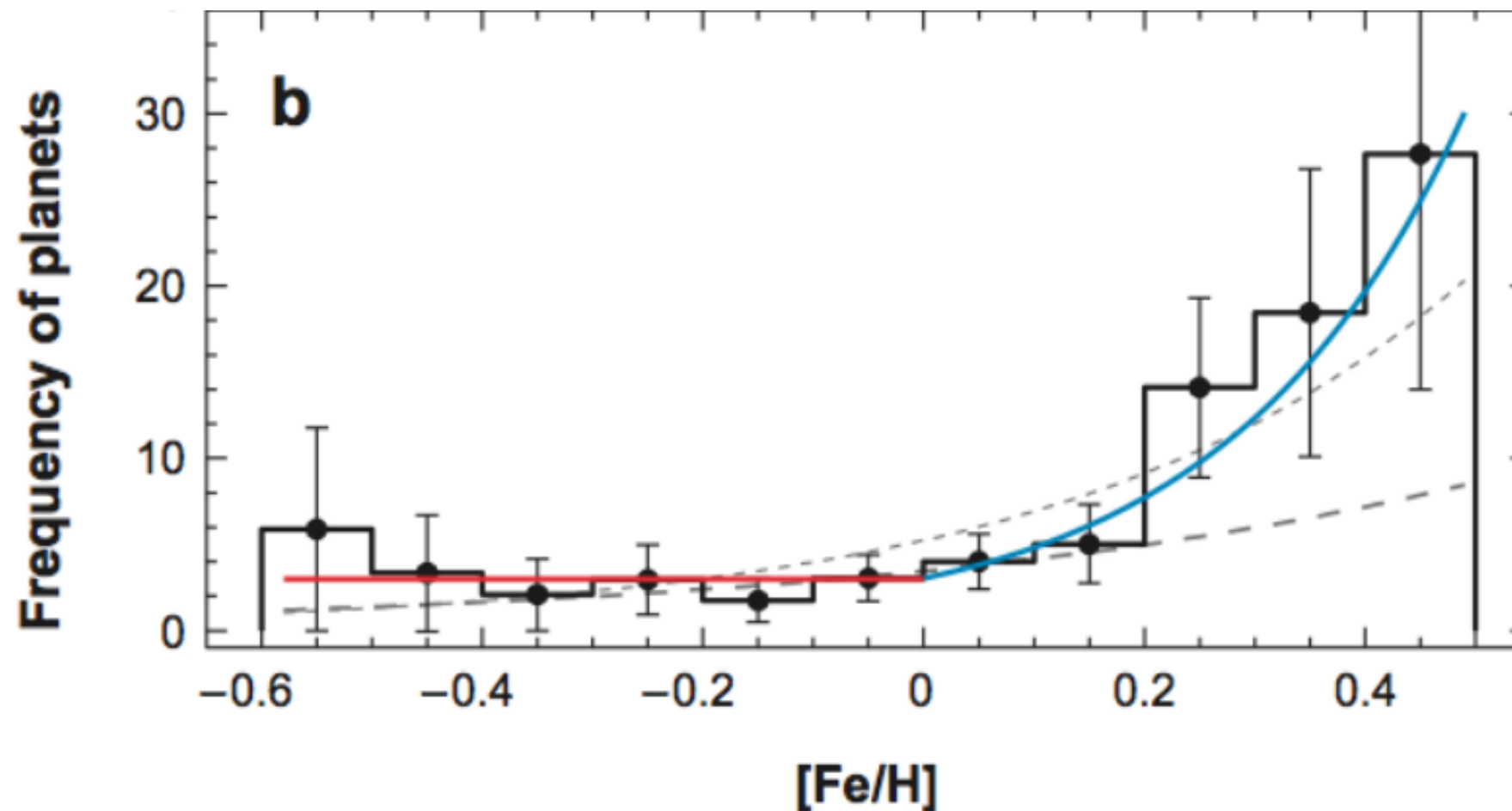
- Pulsar timing
- **Radial velocity**
- **Transits**
- Microlensing
- Direct imaging



Is there any **signature** in chemical composition due to the presence of planets?

Application: Exoplanets

Planets hosts are more metal-rich than average (e.g. Gonzales et al. 1997).



Udry & Santos (2007)

Exoplanets

High-resolution
Mike-Magellan
spectroscopy of **11 solar
twins** and the Sun

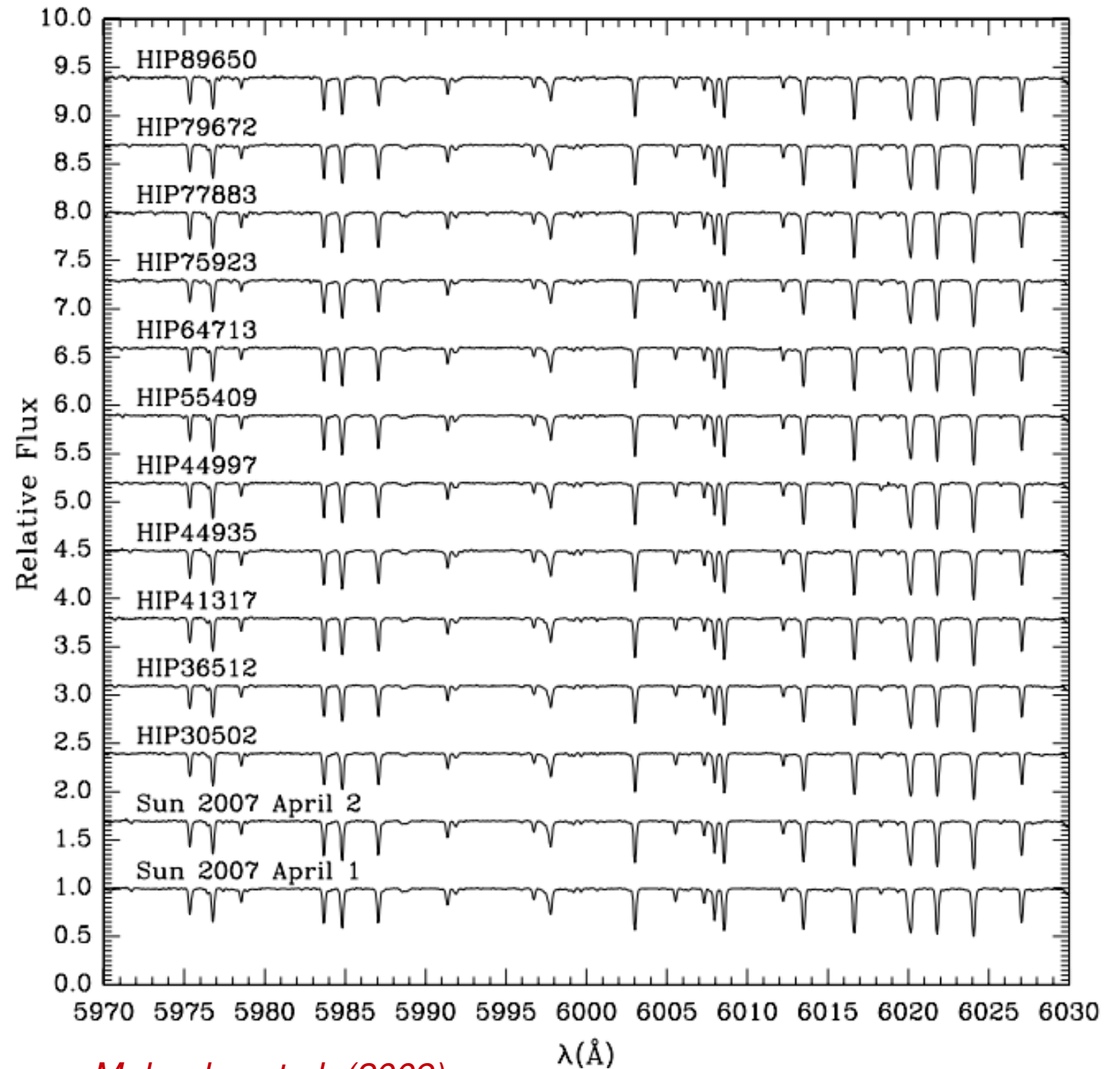
$R=65,000$

$S/N \sim 450$

$\Delta t_{\text{eff}} < 75\text{K}$

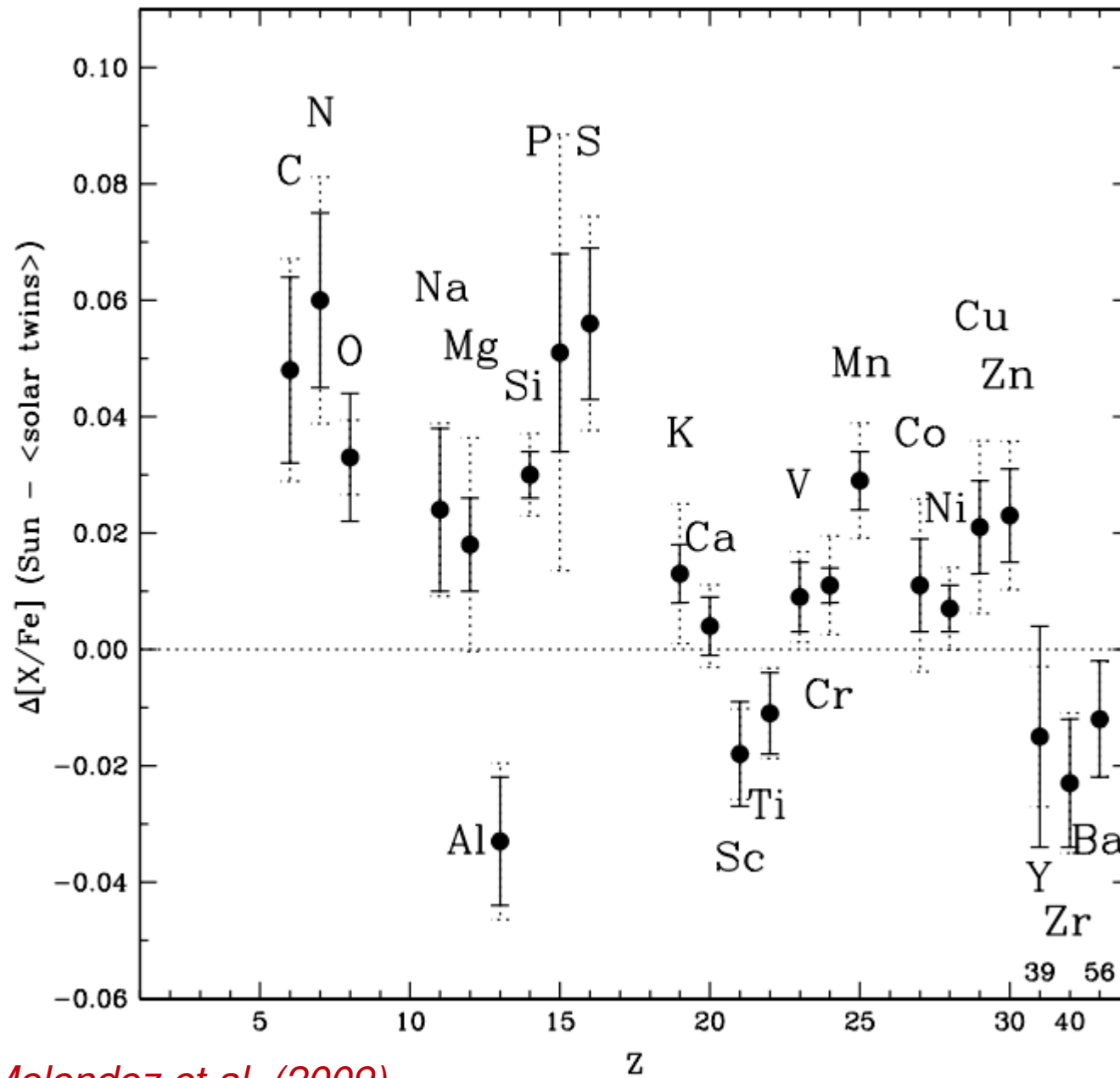
$\Delta \log(g) < 0.1$

$\Delta [\text{Fe}/\text{H}] < 0.1$



Melendez et al. (2009)

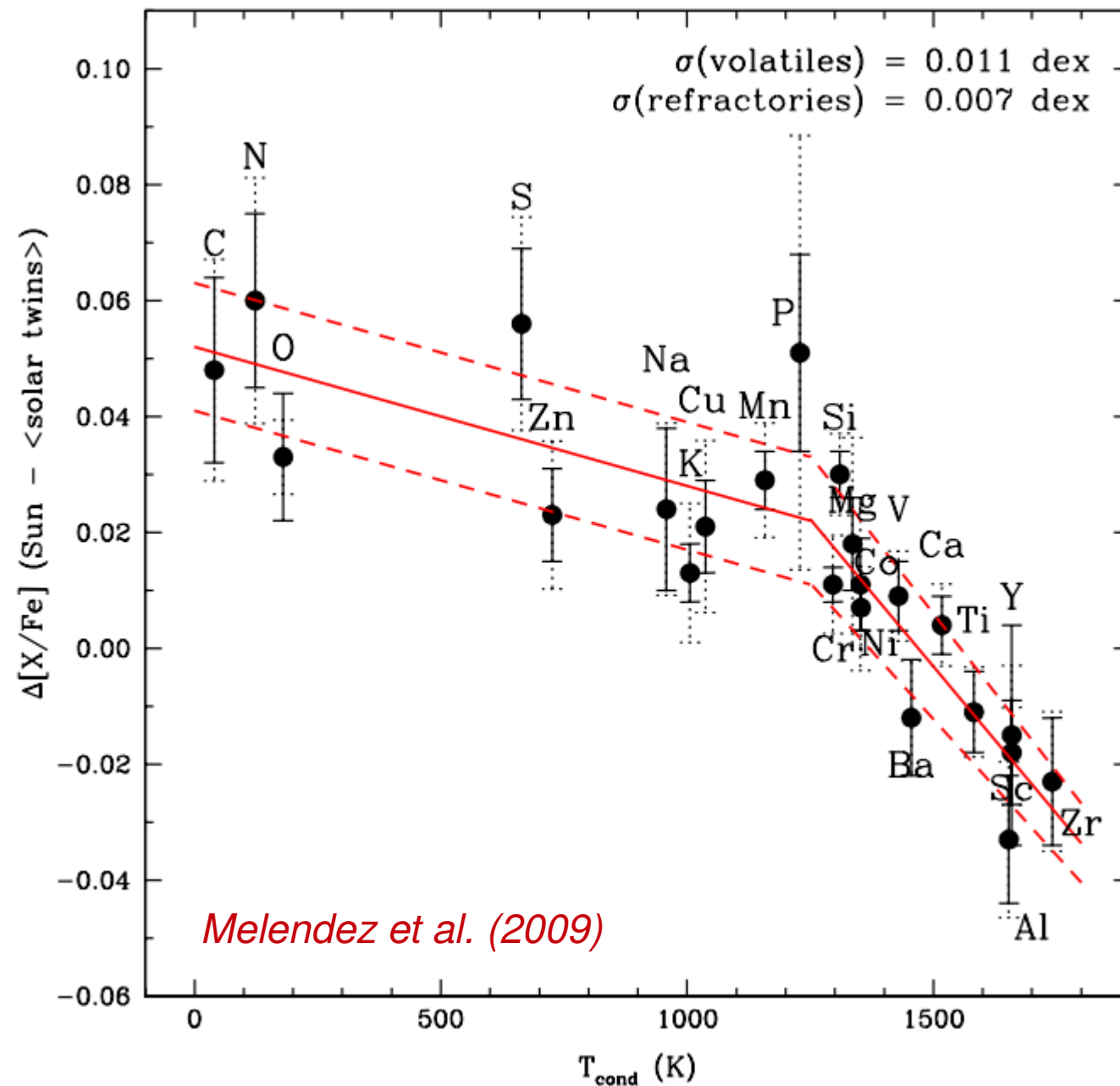
Exoplanets



Melendez et al. (2009)

Precision in stellar spectroscopy is better than **0.01 dex** in $[X/Fe]$ and $[X/H]$.

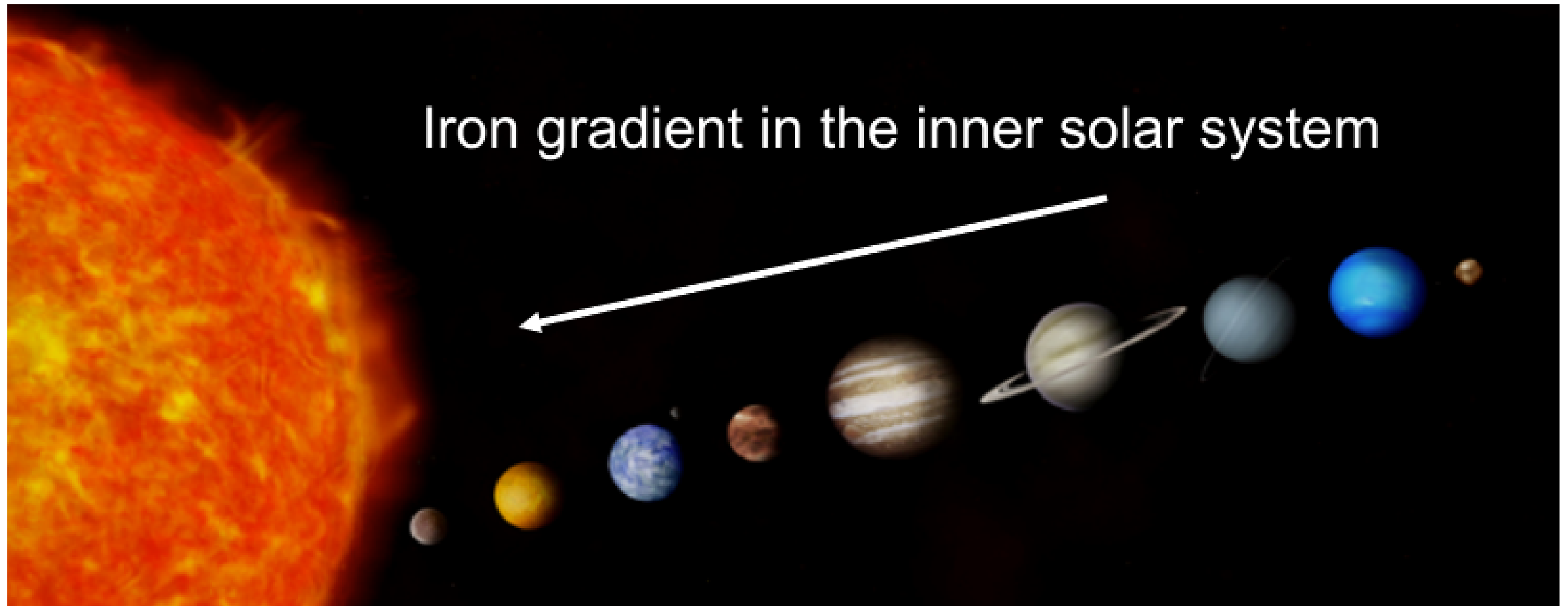
Exoplanets



Highly-significant correlation with **condensation temperature**. Elements that **easily form dust** (with high condensation temperature, i.e., refractories) are underabundant in the Sun. **The Sun unusual !!**

Exoplanets

In the **Sun** planet formation locked up refractories but less of volatiles during the accretion phase.

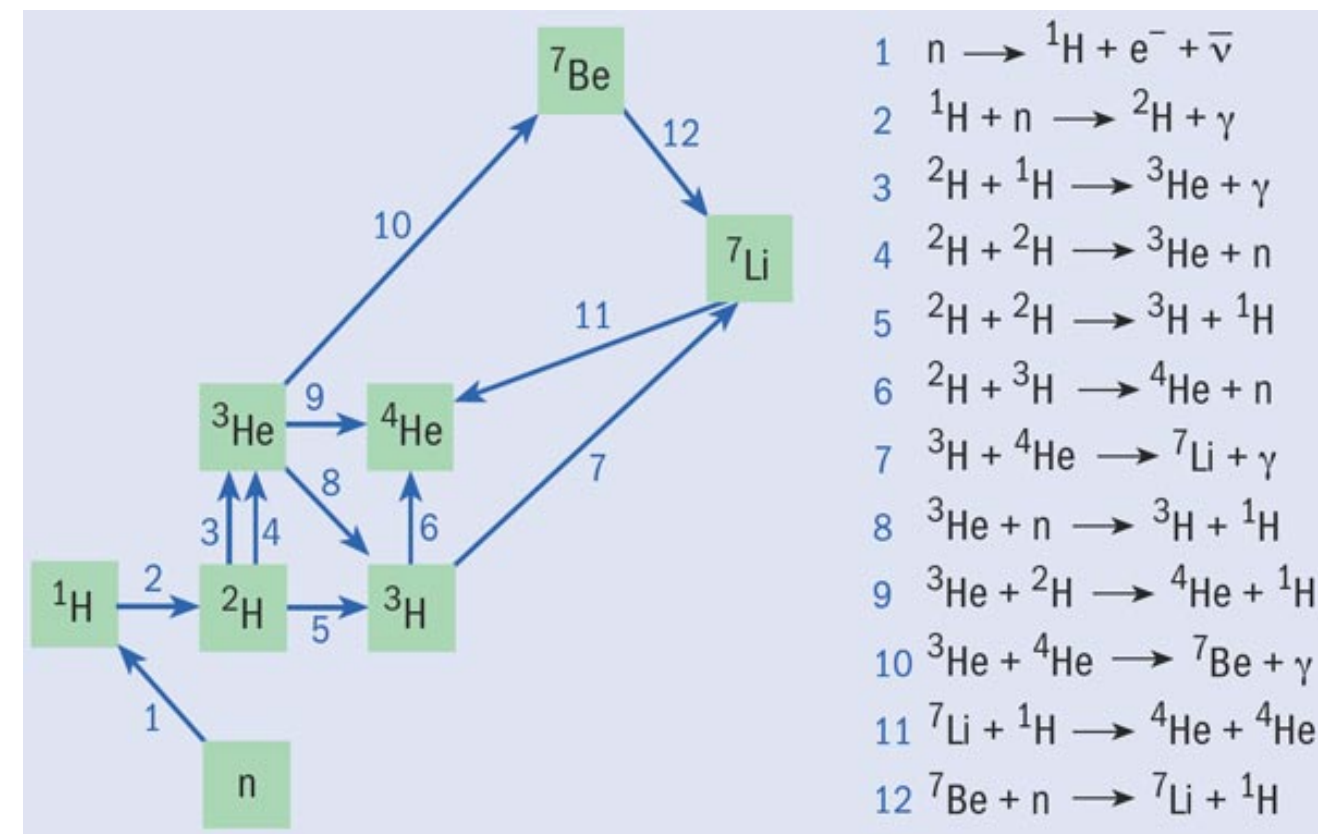


In the **solar twins** there was less planet formation and thus more refractories than Sun.

Application: Testing the elements of the Big Bang

Hydrogen, deuterium and **lithium**, were produced during the **Big Bang nucleosynthesis (BBN)**, when the universe was only a few minutes old.

The present day abundances of Li may depend on the temperatures and densities of the primordial Universe.

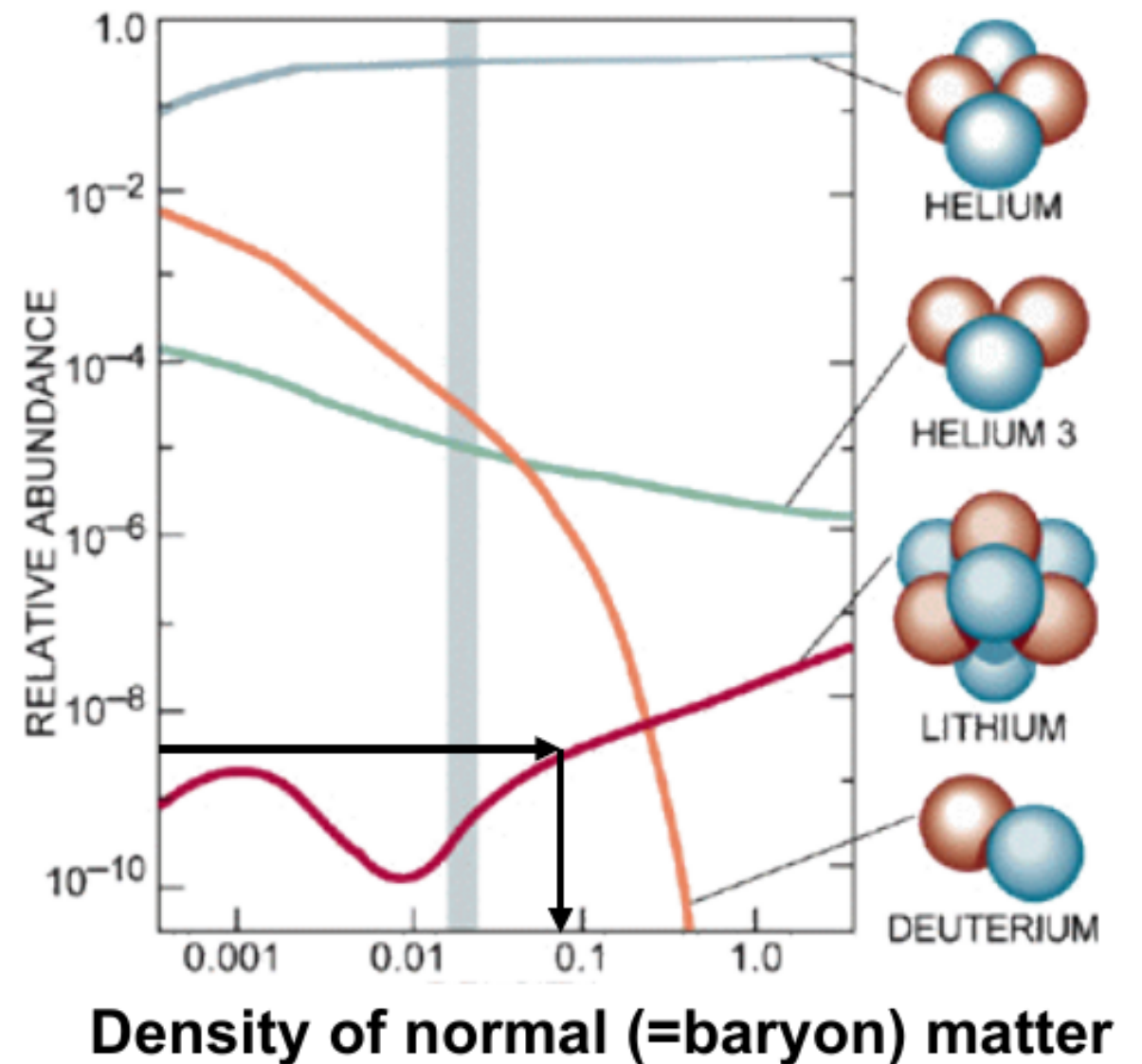


Big-Bang nucleosynthesis

BBN models estimate the mean **baryon density** of the universe.

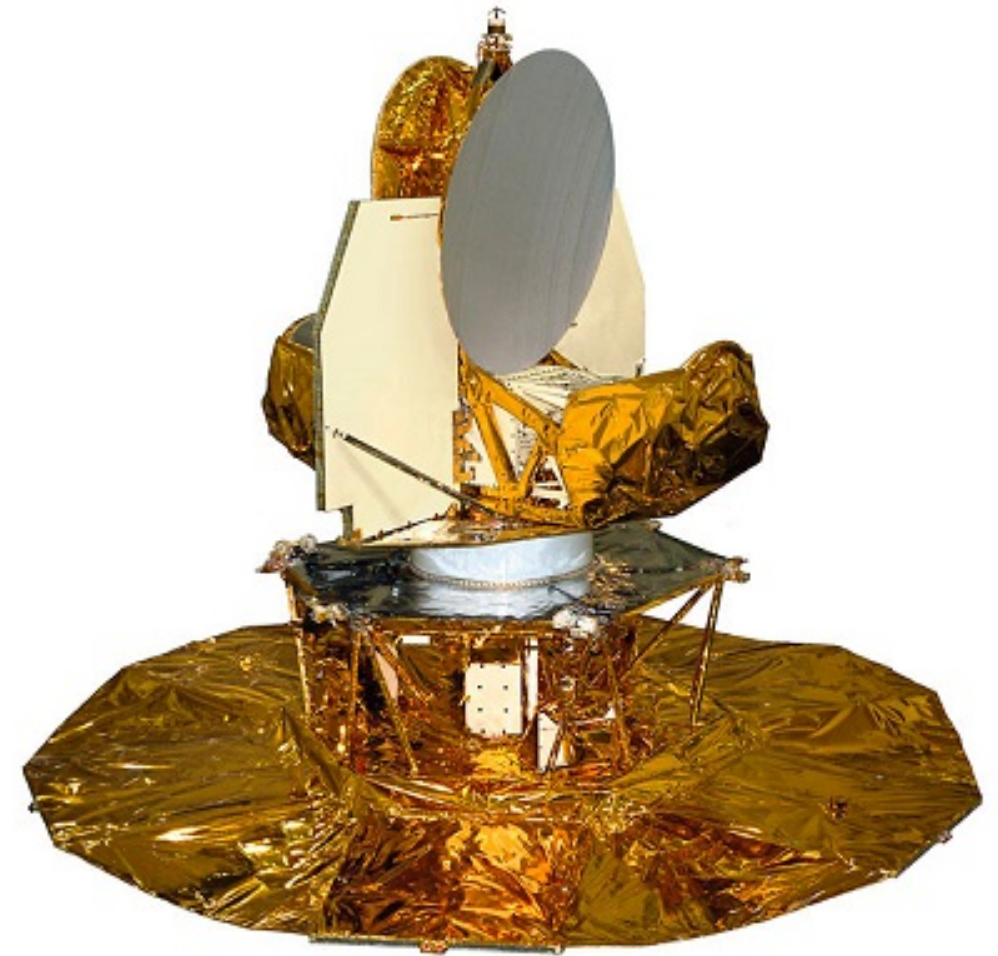
Application: Testing the elements of the Big Bang

The oldest stars may reveal the amount of mass in the Universe



The cosmological lithium problem

Results based on WMAP data conclude that the lithium abundance from Big-Bang nucleosynthesis is **$[A(\text{Li})]=2.72\pm 0.06$** (Dunkley et al. 2009).

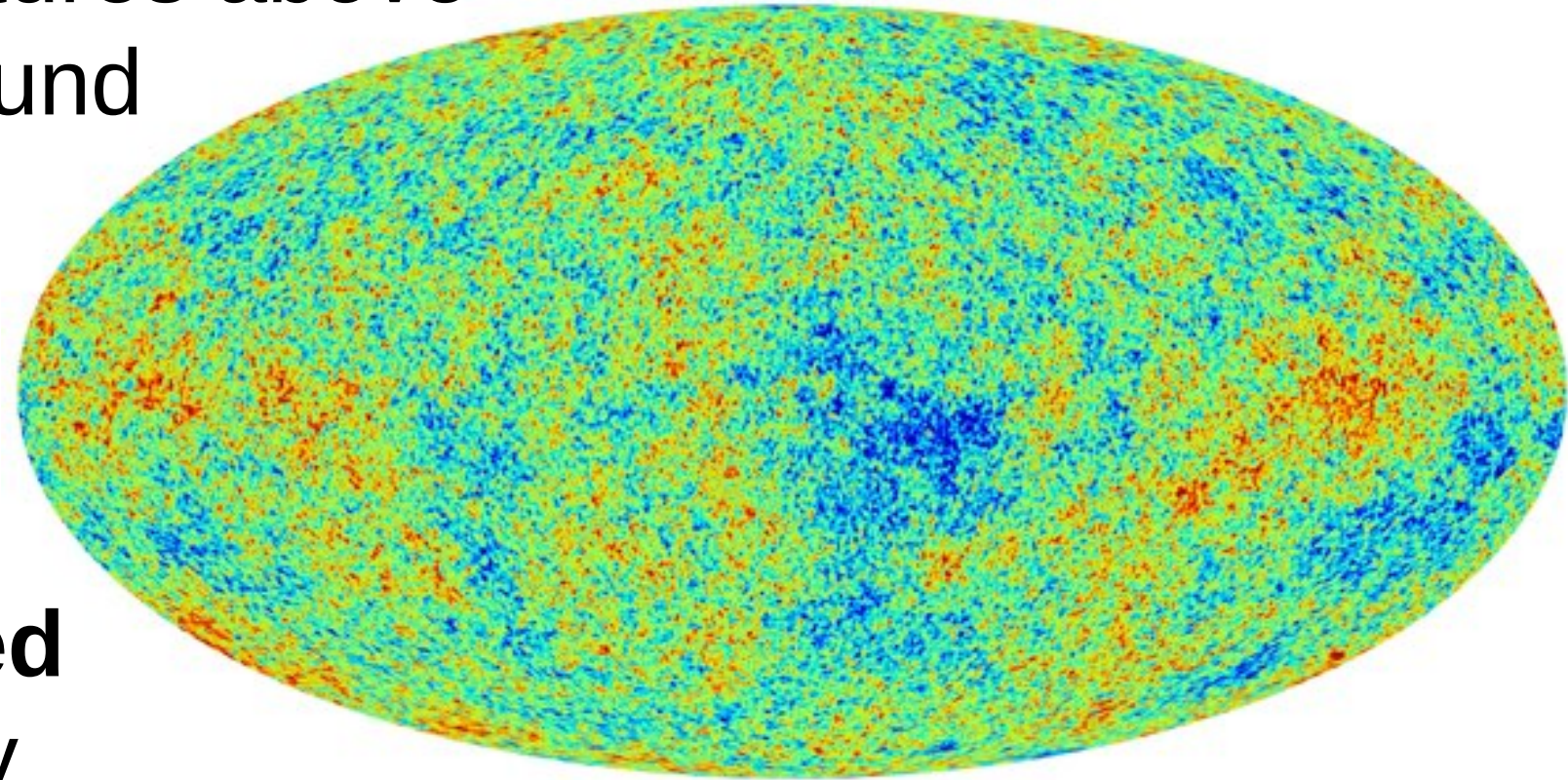


The cosmological lithium problem

Lithium is readily **consumed** by fusion with protons at temperatures above 2×10^6 K, such as is found in the **cores of stars**.

Lithium can be **produced** in **interstellar matter** by collisions with cosmic rays, or by the evolution of **intermediate-mass Stars**.

The lithium abundance in old metal poor stars would correspond to the BBN abundance.



The cosmological lithium problem

- **Nuclear physics in BBNS**

No (e.g. Coc et al. 2002)

- **Stellar T_{eff} -scale**

No (e.g. Casagrande et al. 2010)

- **Stellar atmosphere and line formation**

No (e.g. Asplund et al. 2003; Sbordone et al. 2010)

- **Particle physics in BBNS**

Speculative (many)

- **Stellar Li depletion**

? (e.g. Korn et al. 2006)

The cosmological lithium problem

– Stellar Li depletion

Standard stellar evolution models for Sun and metal-poor turn-off stars do not predict appreciable ${}^7\text{Li}$ depletion

MLT convection zone
not deep enough

Extra mixing due to:

Rotation?

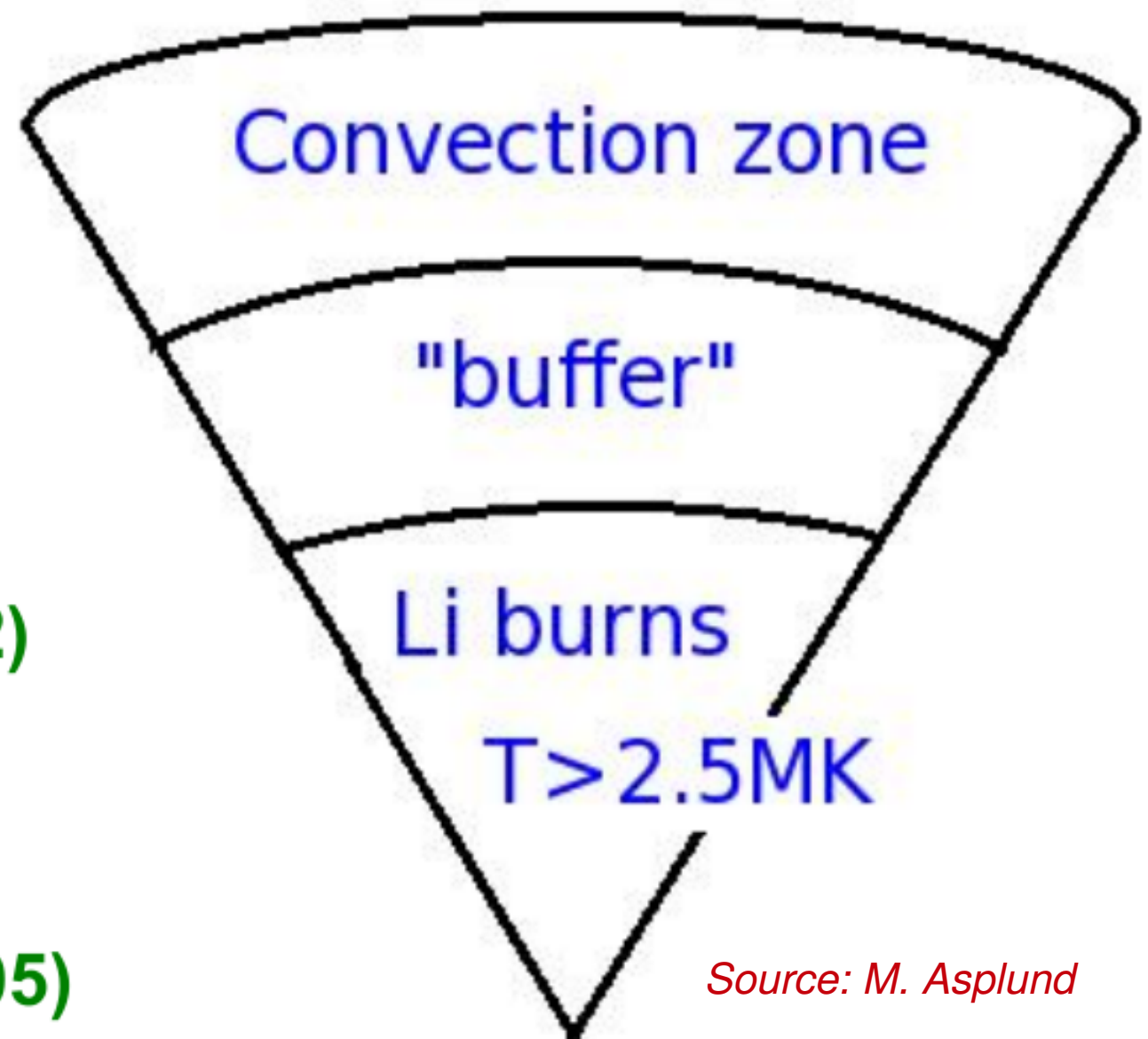
(e.g. Pinsonneault et al. 2002)

Diffusion?

(e.g. Richard et al. 2005)

Gravity waves?

(e.g. Charbonnel & Talon 2005)



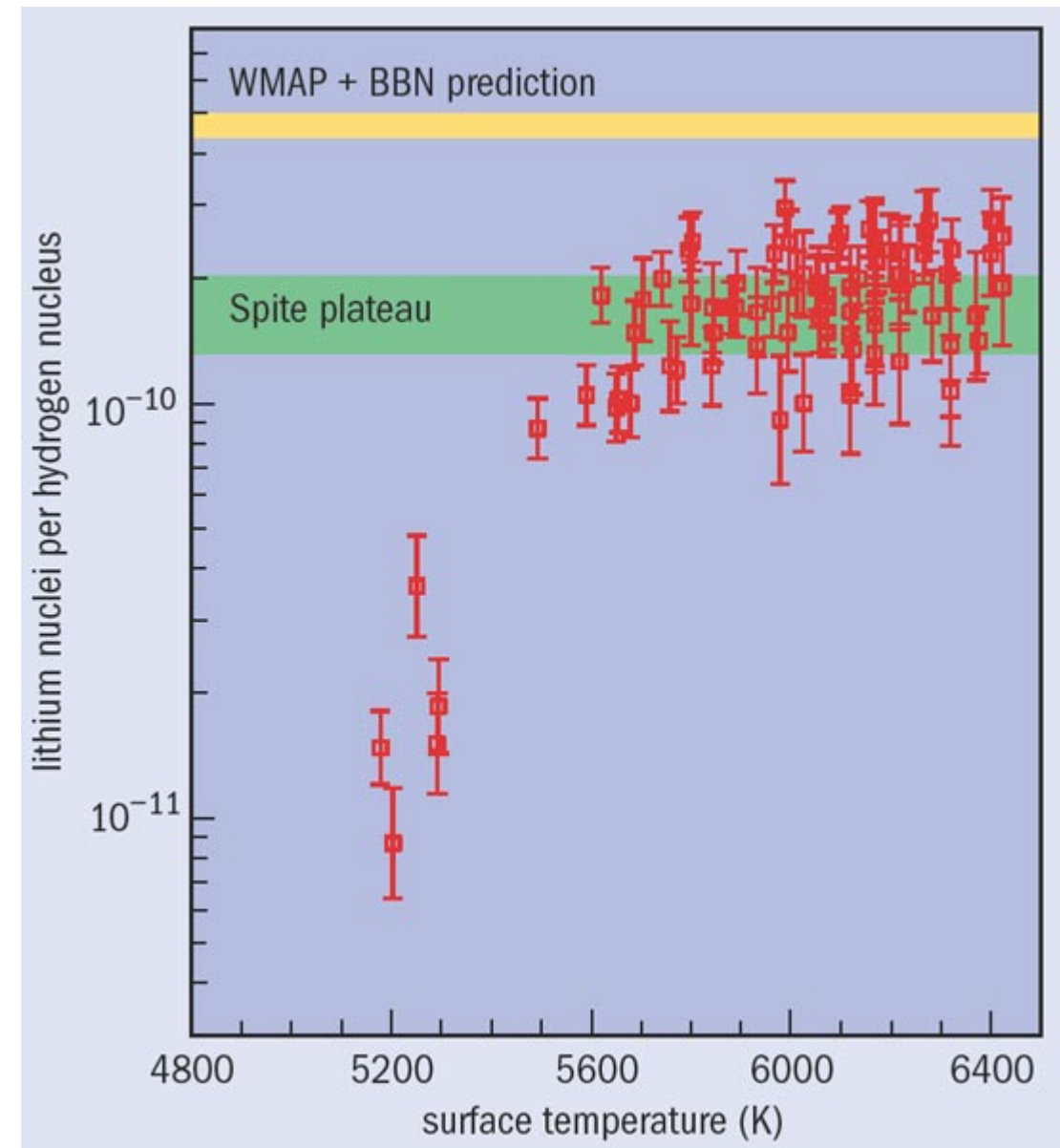
Source: M. Asplund

The cosmological lithium problem

The baseline of the lithium abundance of old stars (or **Spite Plateau**) in the Galactic Halo is significantly lower than what is inferred from WMAP+Big-Bang Synthesis.

Spite & Spite (1982)

This fact is challenging our understanding both of stellar astrophysics and possibly even Big Bang nucleosynthesis itself.



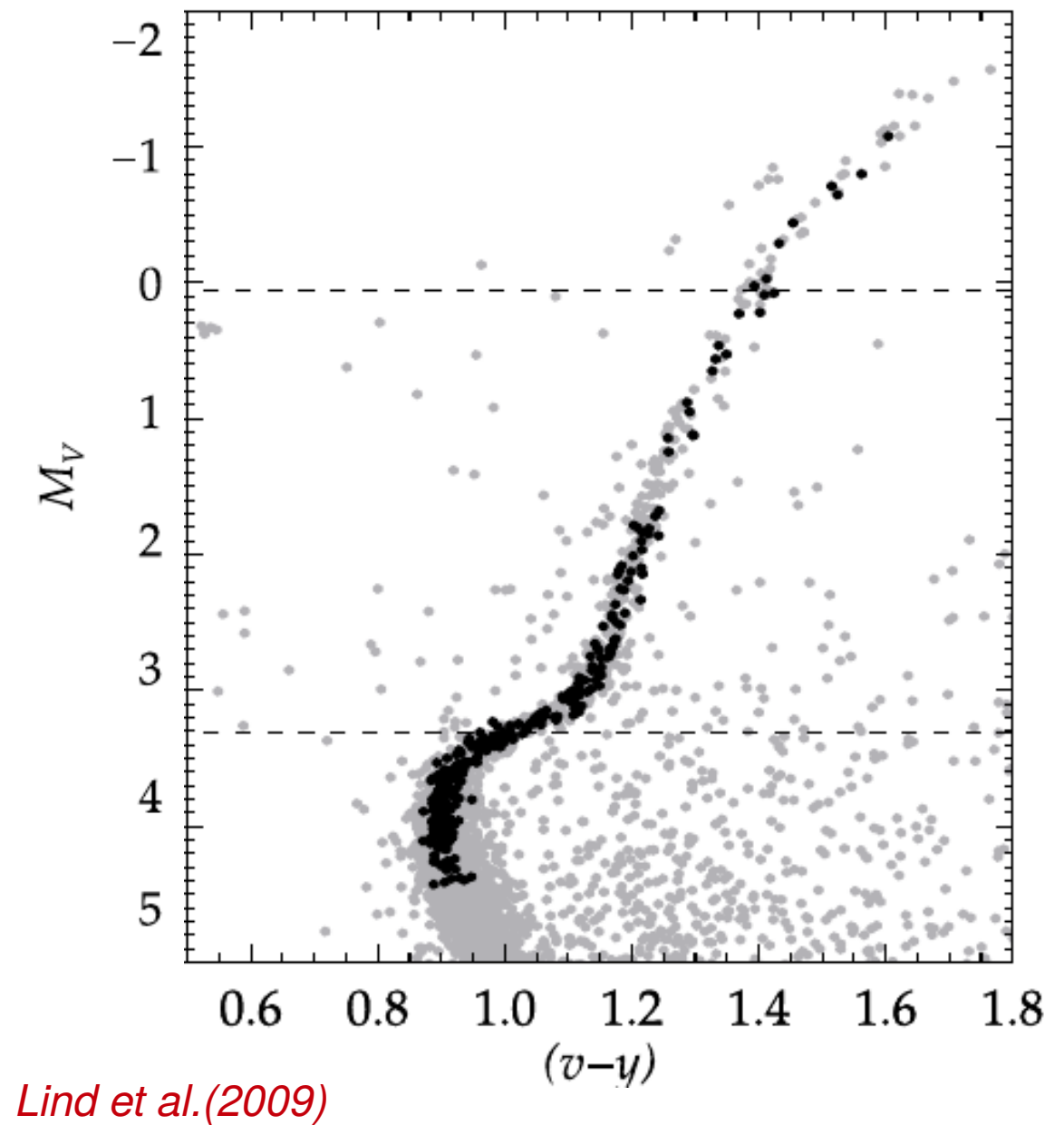
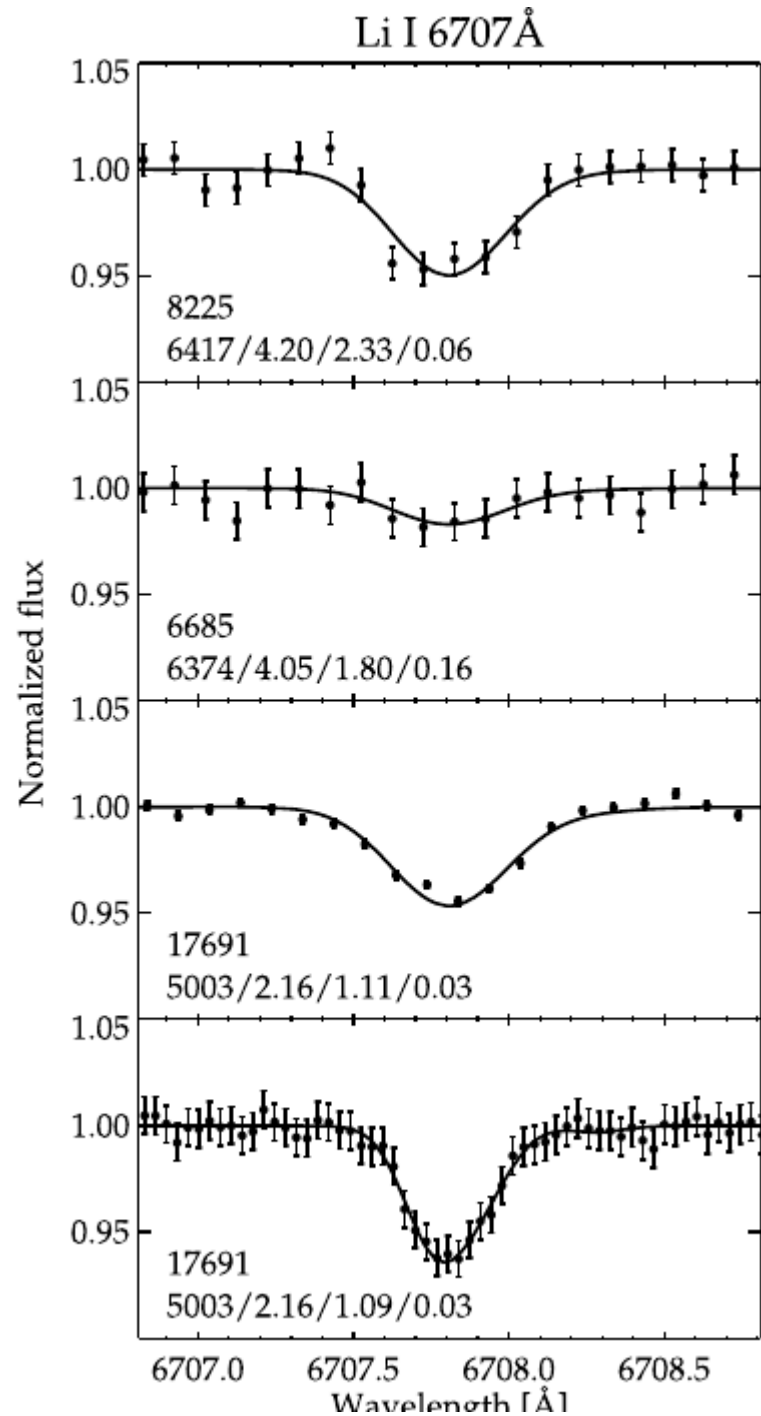
The cosmological lithium problem



Lind et al. (2009)

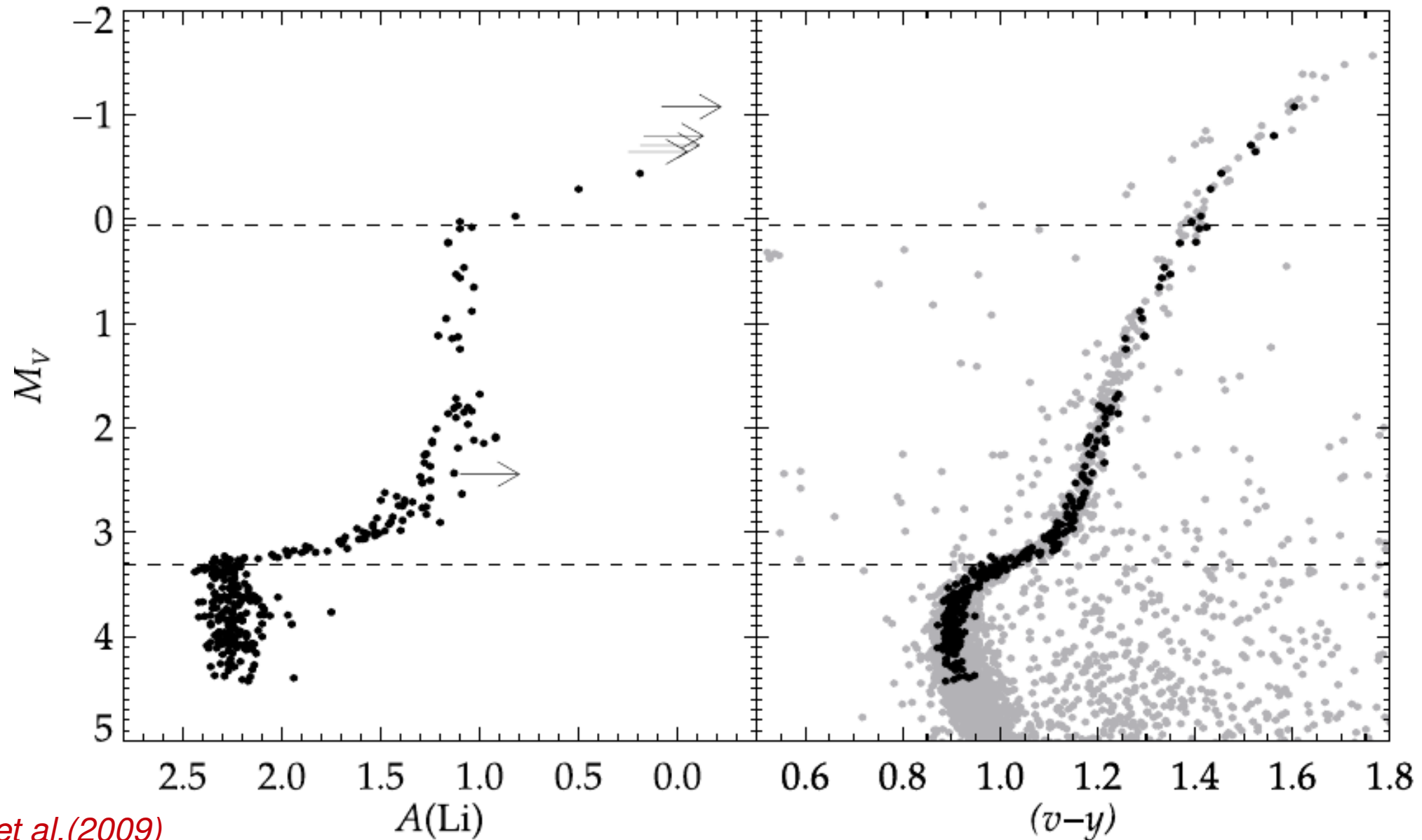
The nearby and metal-poor globular cluster NGC6397 is an ideal object to investigate the cosmological lithium problem

The cosmological lithium problem



Homogeneous analysis of 349 MS, SGB, RGB stars from UVES/GIRAFFE VLT spectra. NLTE analysis.

The cosmological lithium problem

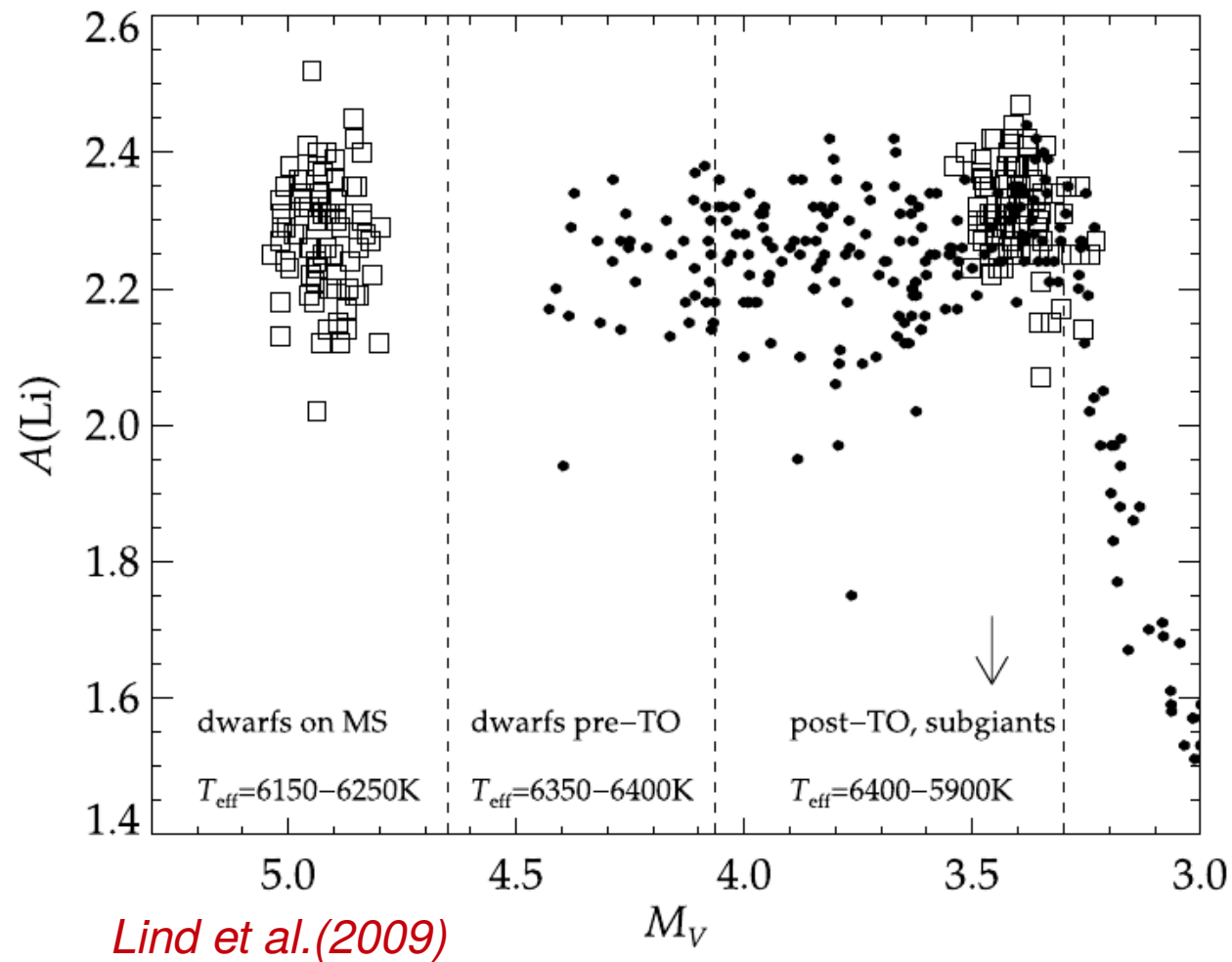


Lind et al. (2009)

Homogeneous analysis of 349 MS, SGB, RGB stars from UVES/GIRAFFE VLT spectra. NLTE analysis.

The cosmological lithium problem

BBN+WMAP



Discrepancy with BBN+WMAP predictions.
Diffusion and **ad-hoc** and turbulence below the convective zone should be invoked to reproduce the observations.